Photocopy and Use Authorization

In presenting this thesis in partial fulfillment of the requirements for an advanced degree at Idaho State University, I agree that the Library shall make it freely available for inspection. I further state that permission for extensive copying of my thesis for scholarly purposes may be granted by the Dean of the Graduate School, Dean of my academic division, or by the University Librarian. It is understood that any copying or publication of this thesis for financial gain shall not be allowed without my written permission.

Signature ___________________________________

Date _______________________________________

Evaluating the influence of irrigation, groundwater, and precipitation on the velocity of Salmon Falls landslide, a slow-moving, rotational slump in southern Idaho.

by

Ian H. Lauer

A thesis

submitted in partial fulfillment

of the requirements for the degree of

Master of Science in Department of Geosciences

Idaho State University

Summer 2018

Committee Approval

To the Graduate Faculty:

The members of the committee appointed to examine the thesis of IAN H. LAUER find it satisfactory and recommend that it be accepted.

Benjamin T. Crosby,
Major Advisor

Glenn D. Thackray,
Committee Member

James M. Mahar,
Graduate Faculty Representative

Dedication

This thesis is dedicated to my beautiful and loving wife Brandi and daughter Sofia. You two are the perfect partners in this journey through life. Thank you Sofia for reminding me we never really have to grow up at heart and Brandi for never encouraging me to.

Acknowledgements

Thank you to all my friends, family, and mentors. You are all authors of this story. For every bit of knowledge gained, wisdom lent, and support given, I am truly grateful.

To my wife Brandi and daughter Sofia, you have been the rock on which I could stand in the rough and raging waters of this river that is life. Your ever-present support, love, and enthusiasm has kept me on course despite life's trials and tribulations.

To all of those who have been mentors in this project, I am ever grateful for the time you take out of your lives to guide us along on ours. Ben, sensei, thank you for taking me into your practice. You have taught me to have confidence in myself and yet a humility in the limit of our individual knowledge. I leave your dojo now but remain a student always. Glenn, your knowledge and guidance in this project has been an invaluable, and I appreciated your ability to always perceive the fine details and connections I missed. I will miss your constant musings and booming voice that could keep me engaged through any talk. James, your insight into this project has been critical and I will never forget there is always an engineering solution to the problem.

Thank you sincerely to the National Science Foundation (Award number: NSF-DUE:1611871) for the generous grant that funded this graduate research and ancillary work. Thanks to UNAVCO for their overwhelming support in completing this work, their part in acquiring funding and equipment, and to Beth Pratt-Sitaula for mentoring me for two summer internships that facilitated the completion of this thesis and the development of associated GETSI curriculum on GPS.

Table of Contents

List of Tables

List of Figures

Evaluating the influence of irrigation, groundwater, and precipitation on the velocity of Salmon Falls landslide, a slow-moving, rotational slump in southern Idaho.

Thesis Abstract - Idaho State University (2018)

The Salmon Falls landslide, a deep-seated rotational slump, previously exhibited the counterintuitive finding of increased sliding velocity during dry summer months, but the suspected attribution to irrigation water was never tested. In this study, we explore drivers of slide velocity at Salmon Falls Creek using contemporaneous daily measurements of GPS positions and water levels. Between 03/2017 and 06/2018, the most consistent, robust predictor of landslide velocity was water level in Bluegill Lake on the slide body, which explained three of four acceleration events. Lake water level was directly associated with initiation and termination of flow in an unlined canal which overflows the canyon rim and supplies the lake. One unexplained acceleration was correlated with a rain-on-snow precipitation event. Regional groundwater failed to explain higher frequency velocity variations. These findings highlight the value of surficial water measurements in predicting landslide velocity and the impact of anthropogenic water redistribution on hillslope stability.

Keywords: slow-moving rotational slump, landslide, pore-water pressure, Salmon Falls Creek, Idaho, canyon formation, geomorphology, hydrogeology, landslide kinematics, static GPS, Global Positioning System, GNSS, irrigation water

Chapter 1: Introduction

1.1 Motivation

Landslides and other mass-wasting events are natural hazards that impact many communities around the world. The impact of these events includes damage to property, infrastructure, and natural resources. The annual global effect of landslides and other mass-wasting events is estimated at 3.5 to 4 billion USD (Singhroy et al., 2000; Danger, 2005) and the loss of approximately 1000 lives (Petley, 2012). In the Unites States, landslides occur in all 50 states, and 29 states list them as one of the top three natural hazards in their area (Highland and Norton, 2006). Understanding the conditions that control landslide initiation and movement is critical in predicting when, where, and how landslides and associated hazards will occur. Due to the complexity of landslide mechanics, local variability in landslide composition and morphology, and modification by human interaction, local or site-specific studies are critical to understanding how landslides will respond in a given environment (Van Asch et al., 1999). In particular, knowledge of landslide-wide kinematics remains somewhat rudimentary, especially in terms of understanding how landslides respond to drivers at various time scales (Schulz et al., 2017), and long term studies for slow moving landslides are particularly rare (Schulz et al., 2009). These observations are important because changes in environmental conditions, such as water inputs, groundwater levels, and temperature, are frequent relative to the duration of the movement, which can last tens to hundreds of years.

In this study, we utilize high precision, daily observation of landslide motion and associated water drivers over the period of one year to answer the following questions regarding the behavior of the Salmon Falls landslide: 1) how does landslide velocity vary temporally over the period of a year? 2) how does landslide velocity vary with changes in water level at a variety of sources? 3) how do various water sources contribute to the greater hydrogeologic setting in the landslide?

1.2 Background

1.2.1 Landslides

Landslides and other mass movements have long been recognized as one of the largest contributors to geomorphic change and are distributed in nearly all high-relief environments. The widespread distribution of landslides contributes to large variability in their physical properties including material composition, slide geometry, and local topographic controls. Additionally, landslides are influenced by geographic and seasonal variation of other known controls such as temperature, precipitation, and pore-water pressure. The complexity of interaction between these various features makes modeling and prediction of landslide activity difficult, but the increasing availability of high precision, high resolution measuring devices allows us to observe these behaviors with increasing reliability.

Fundamentally, landslides and other mass movements are a threshold process that occurs when the driving forces acting on a hillslope exceed the resistive forces acting along a failure surface. The driving force, shear stress, is simply the proportion of gravity acting parallel to the failure surface. In contrast, the resistive forces, or shear strength, of a hillslope is a function of the normal force, cohesion, and friction that opposes stress along a potential failure surface. The shear strength of a hillslope is reduced by the presence of pore-water pressure, which counteracts the normal stress and subsequently reduces friction and cohesion (de Blasio, 2011). Slope stability is often described by the factor of safety, equal to the shear strength divided by shear stress, F_s = Shear Strength / Shear Stress. Slopes are stable when $F_s>1$ and fail when $F_s<=1$. However, this is a highly simplified assessment that only accounts for failure along a single planar failure of known geometry in steady conditions (Figure 1.1). This type of analysis lays the fundamentals from which we can assess how various drivers modify the force balance within landslides.

1.2.2 Rotational Slumps

Rotational slumps are a category of mass movements associated with landslides, but with several distinct characteristics. Slumps are a mass-movement in which the displacement of the slide body is relatively small compared to the length and extent of the failure (Cruden and Varnes, 1996). The initiation of slumps is commonly associated with undercutting of the toe of a slope, and they generally exhibit slow to moderate velocity, from several centimeters to several meters per year, compared to other classifications of slides (Cruden and Varnes, 1996; Hungr et al., 2014). Rotational failures are categorized primarily by a concave-upward curved geometry of the failure surface, which causes rotation of blocks or masses along an axis parallel to the failure surface, rotating and tipping the top edge of blocks backward toward the failure surface (Figure 1.2).

1.2.3 Landslides and Hydrology

One of the most important relationships between environmental drivers and landslides is the correlation between precipitation, subsurface water levels, and landslide movements (Coe et al., 2003; Guzzetti et al., 2008; Schulz et al., 2009; Van Asch et al., 1999). This relationship is complex and driven by several phenomena. First, addition of water to a hillslope increases its total density and mass, thereby increasing the driving force acting parallel with the slope and increasing shear stress. Second, addition of water often modifies the physical characteristics of many materials such as the hydrous expansion of clay, which can cause important cause important reductions in shear strength parameters and are associated with pressure-related feedback cycles (Van Asch et al., 1999). More importantly, water exerts pore pressure along the potential failure surface dependent on depth of the water and degree of saturation. At unsaturated water contents and immediately above water tables, capillary action results in negative pore-pressure that increases the effective stress between grains thereby increasing the shear strength. This interaction is minimized in deep failures but is found to be significant in thin slides and along translational faults (Coe et al., 2003; Schulz et al., 2017; Van Asch et al., 1999). Most importantly for deep-seated failures, saturated water levels exert positive pore-pressure proportional to the hydraulic head. The positive pore-water pressure acts to dilate pore spacing and reduce the effective normal stress and therefore shear strength along a failure surface (Figure 1.1)(Wu and Sidle, 1995). Reduced shear strength reduces the threshold stress needed to initiate and maintain movement on landslides.

Complexities in subsurface hydrology and drivers of groundwater levels are important considerations when determining causal relationships with landslide motion. Fluctuations in pore-water pressure and subsequent alterations of hillslope strength are the cumulative effect of various inputs which operate on multiple time scales. Groundwater levels are found to fluctuate both seasonally, as a function of seasonal water supply, and on shorter, event-based durations such as with high precipitation and rain-on-snow events (Coe et al., 2003; Schulz et al., 2009, 2017). Additionally, these cycles are affected by modification from the built environment such as water withdrawal or input from irrigation and agricultural distribution (Farmer, 2003; Schulz et al., 2009; Bareither et al., 2012). Generally, slow-moving and deep-seated slides are found to be more susceptible to changes in deep saturated water levels and longer-duration, higher-intensity precipitation events (Van Asch et al., 1999; Guzzetti et al., 2008; Vallet et al., 2015) . Whereas their shallow counterparts are susceptible to shorter and lower magnitude precipitation events.

Complexities in the hydrogeology of a landslide additionally complicate investigation of groundwater interaction with slides (Van Asch et al., 1999). Direct measurement of hydraulic head along the failure surface is very difficult in active slides due to difficulties in estimating and placing sensors at the failure surface and the short life of sensors and well locations due to displacement by the slide. Therefore, it is often necessary to estimate the potential pore-water pressure and effective stress based on indirect observations and/or modeling. Groundwater flow paths complicate this assessment because of the potential for complex sub-surface structures (Van Asch et al., 1999). These can cause perched and or confined water systems and modify the potential pressure at depth. Confining geology can act to either insulate failure zones from the presence of perched water tables or increase the pressure due to hydraulic head in a confined system (Angeli, 1992; Rogers and Selby, 1980). The presence of fractures and faults within the slide act as preferential flow paths, increasing pressure. This can be modified by water-material interaction such as the hydrous expansion of clays, which dilate pore spacing, reducing cohesive strength, and also enabling preferential flow along existing failures (Iverson, 2005; Schulz et al., 2017; Van Asch et al., 1999).

1.3 Field Setting

1.3.1 Geology

Salmon Falls Creek incises the Snake River Plain and reveals lithologies typical of the region: lava and volcanic sediments interbedded with sedimentary packages. In the Salmon Falls landslide, the exposed canyon wall is dominantly composed of the Glenns Ferry Formation, part of the greater Idaho Group, which is approximately 1500m thick. The Glenns Ferry formation is a thick sequence of unconsolidated fluvial and lacustrine sediments interbedded with basaltic lava flows and other minor volcanic deposits, approximately 4.5 Ma, which composes the upper-most 600 m stratigraphy of the Snake River Plain proximal to Salmon Falls (Bonnichsen and Godchaux, 2002; Dorsch, 2004; Malde, 1991; Othberg et al., 2012). This includes the Sunset Butte basalt, which likely composes the thickest section of canyon rim which has been displaced in the upper block of the slide (Othberg et al., 2012). The basalt is capped by younger, Pleistocene-age, coarse-grained sediments of the Tuana Gravels, which form a thin, several meter thick section that with the addition of thin aeolian deposits make up the surficial geology in the immediate area (National Park Service, 1999). Most of the historic and active landslides regionally occur along steepened canyon walls in the Glenns Ferry Formation and Yahoo Clay, which is not present at Salmon Falls. Shallow, perched water tables fed by water loss from unlined irrigation systems were attributed to formation of these local landslides in the Hagerman Fossil Beds (Chleborad and Powers, 1996; Farmer, 2003).

1.3.2 Hydrology

The topography of the Snake River plain is defined by wide, flat plains incised by river networks that in its central area form deep, often vertical canyons walls. These canyons often incise below the regional water table and split the Salmon Falls water system from the Eastern Snake River Plain (ESRP) aquifer to the north. Although the ESRP is highly studied, work to the south in our field area is rare and suggests that the area possesses different hydrogeology. Local studies suggest that multiple water tables are present in the Salmon Falls area including perched aquifers, which may develop from infiltration of irrigation water (Chleborad and Powers, 1996; Farmer, 2003; Lewis and Young, 1989). Preliminary work proposed that the upper most productive water table has a relatively consistent elevation, ~1063 m proximal to the landslide, and is contained in the Pliocene sedimentary strata (Lewis and Young, 1989). Both the main aquifer and perched tables are the source of many springs which form along canyon walls and are visible by seepage patterns, vegetation, and occasional discharge (Lewis and Young, 1982).

1.3.3 Salmon Falls Landslide

Salmon Falls landslide is located in south-central Idaho, 10km east of the town of Buhl and along the eastern rim of the canyon of Salmon Falls Creek, a tributary of the Snake River (Figure 1.3). The ca. 5 km long stretch of Salmon Falls canyon along the study area has a geomorphic legacy of mass-wasting events, which has earned it the name of “Sinking Canyon”(Lee, 1938; Dorsch, 2004). Active landslides were reported in the area as early as 1937 (Lee, 1938). Multiple relic landslides are apparent on either side of the canyon, which form steep slopes defined by broken sections of canyon rim basalt. The modern landslide events appear to be reactivations of pre-historic failures, mobilizing old structures as head scarps continue to step back along the canyon rim.

A reactivation of Salmon Falls landslide (also ‘Bluegill landslide’ in early reports) was first reported to local agencies in 1998 by rock climbers concerned by movement in the cliff face. Early assessment suggested that the failure may have reactivated in response to antecedent high precipitation years, although this has yet to be substantiated (Ellis et al., 2004). The slide occurred 0.4 km south of the 1937 slide area, and historical aerial photography suggests that the main surface rupture of the Salmon Falls slide formed simultaneous to failures activated in the 1937 event (Ellis et al., 2004). Based on aerial photography, that rupture remained dormant until the modern slide scarps reactivated along the rupture in the 1990’s. Since its discovery, the Salmon Falls landslide has been the focus of multiple studies focused on quantifying and understanding landslide deformation and the potential for outburst floods on Salmon Falls Creek (Ellis et al., 2004). Current observations reveal it continues to move, and it remains a site of interest and opportunity for landslide kinematics research.

The Salmon Falls landslide is a slow-moving, rotational slump (Cruden and Varnes, 1996) composed of multiple blocks of canyon rim basalt that lie over unconsolidated silt, sand, gravel, and minor interbedded basalt of the Pliocene age Glenns Ferry Formation. Several large blocks of the basalt have failed above the sedimentary package and rotated down and west into the canyon (Figure 1.3)(Dorsch, 2004). Early GPS, theodolite, and extensometer measurements recorded rapid movement up to 2-4 cm/month in November 2001, which subsequently decreased to slow, continuous deformation between 10-15 cm/yr (Chadwick, Thackray, et al., 2005; Dorsch, 2004; Ellis et al., 2004). The total displacement is relatively small with respect to the size of the slide; only 10s of meters of movement have occurred along the 500m length of the slide in 20 years.

Initial observations and kinematic assessment were conducted with GPS (Chadwick, Dorsch, et al., 2005; Dorsch, 2004), LiDAR (Glenn et al., 2006), InSAR (Necsoiu et al., 2014), and experimental wireless positioning sensors (Kenney et al., 2009). GPS surveying revealed differential movement across the body of the slide as well as temporal variation in landslide velocity, as shown in Figure 1.4. An acceleration in landslide velocity was recorded at this time, but equipment shortcomings caused large data gaps. Additionally, kinematic assessment concluded that landslide could be divided into three distinct sections, the upper block, the middle, and the toe (Figure 1.3). The bulk movement of the slide is down and to the west, failing along a hypothesized rotational detachment (Dorsch, 2004; Necsoiu et al., 2014). The upper block is a relatively massive section of basalt and underlying sediment which detached from the canyon rim and is bounded by the current active scarp along the east and by a second scarp and talus field to the west. The upper block has moved down and west, although large sections have begun to separate and deviate with movement to the north. The main body of the slide, which is located below the talus slope and west of the upper block, translates to the west with negligible vertical displacement. The toe of the slide is the westernmost section identified by its distinct upward displacement and damming of Salmon Falls Creek.

Several distinct water features exist in the area (Figure 1.5). First, Bluegill Lake is elevated upon the landslide body, although its existence pre-dates the slide formation. The lake exists year-round, to our best observation, but has no apparent surficial sources (Figure 1.5). Additionally, several springs emerge from the face of the talus slope immediately below the main slide block, above Bluegill Lake, and along the eastern slope of the dammed section of Salmon Falls Creek. Over the last 19 years, the dam has been relatively stable, although its outlet has migrated since the mid 2000's. The large volume of water impounded behind the dam in Salmon Falls Creek caused concern for outbreak flooding of homes and recreational sites downstream, although this has since been deemed relatively safe (Ellis et al., 2004).

Since its initial characterization in the early 2000's, work has continued sporadically. Repeat aerial LiDAR was collected in 2005 and 2011, although presently it has only been used as a sample dataset for methodological testing (Glenn et al., 2006)Most recently, starting in 2015 periodic RTK GPS surveys have been taken at approximately 80 pin-type monuments on the slide, confirming continued motion of the slide and providing greater spatial context to the new static GPS campaigns (pers. comm. Benjamin T. Crosby).

1.4 Impetus

Although the Salmon Falls site is well-studied, and its occurrence is undoubtedly a natural stage of canyon evolution in this environment, questions remain as to what controls landslide motions in this area and if this new information will be able to improve management of the area. Multiple previous authors have suggested that groundwater contribution may be controlling the velocity of the slide due to the effect of pore-water pressure, a known relationship in landslide mechanics (Ellis et al., 2004; Dorsch, 2004; Chadwick, Dorsch, et al., 2005; Necsoiu et al., 2014). Landslides are the common mechanism for canyon formation along the Snake River plain and analogous regions, but these events have been proposed to be accelerated by or prematurely initiated from incidental loss of irrigation water (Chleborad and Powers, 1996; Farmer, 2003; Hays et al., 1982; Bareither et al., 2012). Due to the timing of landslide activity, which is highest in the summer, anthropogenic water sources, such as a canal parallel to the canyon rim, have been questioned as a possible a source. Local mass-wasting in the Hagerman Fossil beds, 40km to the north east and located in the same geologic setting, was attributed to locally elevated groundwater systems caused by irrigation loss on unlined canals (Chleborad and Powers, 1996; Farmer, 2003).

In addition to local value, knowledge of kinematics and control of deep-seated, slow, rotational failure is relatively limited (Schulz et al., 2009, 2017) and the USGS lists the development of predictive models for large, slow moving landslides as one of their major research priorities in the field (Danger, 2005). Long-term studies of landslide kinematics and controls is an invaluable asset to this and future research. As such, observation of the Salmon Falls landslide presented an opportunity to both reassess the stability of the slide and investigate lingering questions of which water impacts landslide velocity.

In this study, we investigated the primary controls of landslide activity and the kinematics of the Salmon Falls landslide, by utilizing continuous high-precision observation of both GPS and known environmental drivers. We reoccupy the previously existing campaign locations from the 2003 survey along with several new stations to assess current landslide motion. This network of seven semi-permanent, static GPS systems was used to produce sub-cm precision, daily resolution time-series of landslide motion across the active slide.

Landslide velocity is then compared with contemporaneous observation of multiple potential environmental drivers. In particular, we assess the influence of multiple potential water sources that may be responsible for elevating local groundwater levels and subsequently pore-water pressure, a known driver of landslide activity (Chleborad and Powers, 1996; Coe et al., 2003; Schulz et al., 2009, 2017; Záruba and Mencl, 2014; Van Asch et al., 1999). Potential water contributions to the slide are assessed using three local water tables, an irrigation canal, precipitation records, and then analyzed for temporal correlation to landslide velocity.

Through these observations we find that landslide motion does vary throughout the period of one year and is consistent between multiple stations distributed on the landslide. We observe similarities between the time series of GPS velocity and water levels.

These findings contribute to the overall understanding of landslide activity in this region and provide high temporal resolution information on how landslides behave in this setting. These findings will also be relevant to many analogous canyon formation processes along the Snake River Plain, Idaho, Oregon, and Washington (Farmer, 2003; Malde, 1991; Markley, 2013; Othus, 2008; Safran et al., 2015). Additionally, these results will add to the current breadth of literature on temporal and spatial variation in landslide kinematics for similar types of mass movements, of which slow-moving rotational slumps are generally underrepresented in current literature (Gokceoglu and Sezer, 2009).

1.5 Thesis Structure

This thesis is divided into three chapters. This introductory chapter presents the project motivation, setting, and a summary of key findings. The second chapter is a stand-alone paper addressing the primary component of work in a publication-ready format. The last chapter concludes the thesis with a broader interpretation of results, implications for the work, and suggestions for future project directions.

References

Angeli, M.G., 1992, Observed and predicted critical hydraulic conditions in natural inhomogeneous slopes, *in* Chowdhury, R, N., ed., Geomechanics and Water Engineering in Environmental Management: London, England, Routledge, p. 103–165.

Van Asch, T.W.J., Buma, J., and Van Beek, L.P.H., 1999, A view on some hydrological triggering systems in landslides: Geomorphology, v. 30, p. 25–32, doi: 10.1016/S0169-555X(99)00042-2.

Bareither, C.A., Edil, T.B., and Benson, C.H., 2012, Investigation of White Bluffs Landslides in Washington State: GeoCongress 2012: State of the Art and Practice in Geotechnical Engineering, 2012, p. 546–555, doi: 10.1061/9780784412121.057

De Blasio, F.V., 2011, Introduction to the Physics of Landslides: lecture notes on the dynamics of mass wasting: Springer, 408 p., doi: 10.1007/978-94-007-1122-8.

Bonnichsen, B., and Godchaux, M.M., 2002, Late Miocene, Pliocene, and Pleistocene geology of southwestern Idaho with emphasis on basalts in the Bruneau--Jarbidge, Twin Falls, and western Snake River Plain regions: Tectonic and Magmatic Evolution of the Snake River Plain Volcanic Province: Idaho Geological Survey Bulletin, v. 30, p. 233–312.

Chadwick, D.J., Dorsch, S.J., Glenn, N.F., Thackray, G.D., and Shilling, K., 2005, Application of multi-temporal high-resolution imagery and GPS in a study of the motion of a canyon rim landslide: Photogrametry and Remote Sensing, v. 59, p. 212–221, doi: 10.1016/j.isprsjprs.2005.02.001.

Chadwick, D.J., Thackray, G.D., and Glenn, N.F., 2005, Landslide Surveillance : New Tools for an Old Problem: Eos, Transactions American Geophysical Union, v. 86, p. 109–120, doi: 10.1029/2005EO110001

Chleborad, A.F., and Powers, P.S., 1996, Slope map and locations of irrigation-induced landslides and seepage areas, Hagerman Fossil Beds National Monument, Idaho: U.S. Geological Survey Open-File Report 96-258, 1 p., http://pubs.er.usgs.gov/publication/ofr96258.

Coe, J.A., Ellis, W.L., Godt, J.W., Savage, W.Z., Savage, J.E., Michael, J.A., Kibler, J.D., Powers, P.S., Lidke, D.J., and Debray, S., 2003, Seasonal movement of the Slumgullion landslide determined from Global Positioning System surveys and field instrumentation, July 1998 – March 2002: Engineering Geology, v. 68, p. 67–101, doi: 10.1016/S0013-7952(02)00199-0.

Cruden, D.M., and Varnes, D.J., 1996, Landslide Types and Processes, *in*: Turner, A.K., Schuster, R.L., eds., Landslides: investigation and mitigation, National Research Council, Transportation Research Board Special Report, v. 247: Washington, D.C., National Academy Press, p. 36-75

Danger, A.N., 2005, Landslide Hazards — A National Threat, Landslide potential of the conterminous United States: U.S. Geological Survey Fact Sheet 2005-3156, 2 p. https://pubs.usgs.gov/fs/2005/3156/2005-3156.pdf.

Dorsch, S.J., 2004, The Geologic framework, movement history and mechanics of the Salmon Falls Landslide, Twin Falls County, Idaho [M.S. thesis]: Idaho State University, 138 p.

Ellis, W.L., Schuster, R.L., and Schulz, W.H., 2004, Assessment of hazards associated with the Bluegill Landslide, South-Central Idaho: U.S. Geological Survey Open-File Report 2004-1054. 16 p.

Farmer, N., 2003, Hagerman Valley landslides triggered by land-use change endanger lives, and destroy natural and cultural resources (Hagerman Valley Fossil Beds National Monument, NPS, Idaho): Journal of the Japan Landslide Society, v. 40, p. 341–343, doi: 10.3313/jls.40.4_341.

Glenn, N.F., Streutker, D.R., Chadwick, D.J., Thackray, G.D., and Dorsch, S.J., 2006, Analysis of LiDAR-derived topographic information for characterizing and differentiating landslide morphology and activity: Geomorphology, v. 73, p. 131–148, doi: 10.1016/j.geomorph.2005.07.006.

Gokceoglu, C., and Sezer, E., 2009, A statistical assessment on international landslide literature (1945-2008): Landslides, v. 6, p. 345–351, doi: 10.1007/s10346-009-0166-3.

Guzzetti, F., Peruccacci, S., Rossi, M., and Stark, C.P., 2008, The rainfall intensity-duration control of shallow landslides and debris flows: An update: Landslides, v. 5, p. 3–17, doi: 10.1007/s10346-007-0112-1.

Hays, W.H., Schuster, R.L., Neumann, H.D., and Harrod, G.W., 1982, Active landslides on the White Bluffs of the Columbia River, south-central Washington: Geologic Society of America, v. 14, p. 1–71.

Highland, L.M., and Norton, G., 2006, Estimating Landslide Losses — Preliminary Results of a Seven-State Pilot Project: U.S. Geological Survey Open-File Report 2006-1032, 11 p.

Hungr, O., Leroueil, S., and Picarelli, L., 2014, The Varnes classification of landslide types, an update: Landslides, v. 11, p. 167–194, doi: 10.1007/s10346-013-0436-y.

Iverson, R.M., 2005, Regulation of landslide motion by dilatancy and pore pressure feedback: Journal of Geophysical Research: Earth Surface, v. 110, 16 p., doi: 10.1029/2004JF000268.

Kenney, J.D., Poole, D.R., Willden, G.C., Abbott, B.A., Morris, A.P., McGinnis, R.N., and Ferrill, D.A., 2009, Precise positioning with wireless sensor nodes: Monitoring natural hazards in all terrains, *in* 2009 IEEE International Conference on Systems, Man and Cybernetics: San Antonio, TX , p. 722–727, doi: 10.1109/ICSMC.2009.5346714

Lee, C.A., 1938, Recent Landslides in Salmon Creek Canyon, Idaho: The Journal of Geology, v. 46, p. 660–665, doi: 10.1086/624667

Lewis, R.E.E., and Young, H.W., 1982, Geothermal resources in the Banbury Hot Springs area, Twin Falls County, Idaho: U.S. Geological Survey Water Supply Paper 2186, v. 27, 32 p.

Lewis, R.E., and Young, H.W., 1989, The hydrothermal system in central Twin Falls County, Idaho: U.S. Geological Survey Water-Resources Investigation Report 88-4152, 44 p.

Malde, H.E., 1991, Quaternary geology and structural history of the Snake River Plain, Idaho and Oregon: The Geology of North America, v. 2, p. 251–281.

Markley, C.E., 2013, Characterization of mass wasting through the spectral analysis of LiDAR imagery: Owyhee River, Southeastern Oregon [M.S. thesis]: Central Washington University. 60 p.

Necsoiu, M., McGinnis, R.N., and Hooper, D.M., 2014, New insights on the Salmon Falls Creek Canyon landslide complex based on geomorphological analysis and multitemporal satellite InSAR techniques: Landslides, v. 11, p. 1141–1153, doi: 10.1007/s10346-014-0523-8.

National Park Service, 1999, Revised Resources Management Plan Hagerman Fossil Beds National Monument, ID: National Park Service HAFO, https://www.nps.gov/hafo/learn/management/interp-goals.htm%0A.

Othberg, K.L., Kauffman, J.D., Gillerman, V.S., Garwood, D.L., 2012, Geologic Map of the Twin Falls 30 x 60 Minute Quadrangle , Idaho: Idaho Geological Survey Map 49, scale 1:100,000.

Othus, S.M., 2008, Comparison of Landslides and Their Related Outburst Flood Deposits, Owyhee River, Southeastern Oregon [M.S. theis]: Central Washington University, 146 p.

Petley, D., 2012, Global patterns of loss of life from landslides: Geology, v. 40, p. 927–930, http://dx.doi.org/10.1130/G33217.1.

Rogers, N.W., and Selby, M.J., 1980, Mechanisms of shallow translational landsliding during summer rainstorms: North Island, New Zealand: Geografiska Annaler, Series A, Physical Geography, v. 62, p. 11–21, doi: 10.1080/04353676.1980.11879995

Safran, E.B., O'Connor, J.E., Ely, L.L., House, P.K., Grant, G.E., Harrity, K., Croall, K., and Jones, E., 2015, Plugs or flood-makers? the unstable landslide dams of eastern Oregon: Geomorphology, v. 248, p. 237–251, doi: 10.1016/j.geomorph.2015.06.040.

Schulz, W.H., Coe, J.A., Ricci, P.P., Smoczyk, G.M., Shurtleff, B.L., and Panosky, J., 2017, Landslide kinematics and their potential controls from hourly to decadal timescales: Insights from integrating ground-based InSAR measurements with structural maps and long-term monitoring data: Geomorphology, v. 285, p. 121–136, doi: 10.1016/j.geomorph.2017.02.011.

Schulz, W.H., McKenna, J.P., Kibler, J.D., and Biavati, G., 2009, Relations between hydrology and velocity of a continuously moving landslide-evidence of pore-pressure feedback regulating landslide motion: Landslides, v. 6, p. 181–190, doi: 10.1007/s10346-009-0157-4.

Singhroy, V.H., Loehr, J.E., and Correa, A.C., 2000, Landslide risk assessment with high spatial resolution remote sensing data, *in* Proceedings, IGARSS 2000, IEEE International Geoscience and Remote Sensing Symposium: Honolulu, Hawaii, v. 6, doi: 10.1109/IGARSS.2000.859620

Vallet, A., Bertrand, C., Fabbri, O., and Mudry, J., 2015, An efficient workflow to accurately compute groundwater recharge for the study of rainfall-triggered deep-seated landslides, application to the Séchilienne unstable slope (western Alps): Hydrology and Earth System Sciences, v. 19, p. 427–449, doi: 10.5194/hess-19-427-2015

Wu, W., and Sidle, R.C., 1995, A distributed slope stability model for steep forested basins: Water Resources Research, v. 31, i. 8, p. 2097–2110, doi: 10.1029/95WR01136

Záruba, Q., and Mencl, V., 2014, Landslides and their control: Developments in Geotechnical Engineering: v. 31, e. 2, 324 p., doi: 10.1016/0013-7952(73)90037-9.

Figures

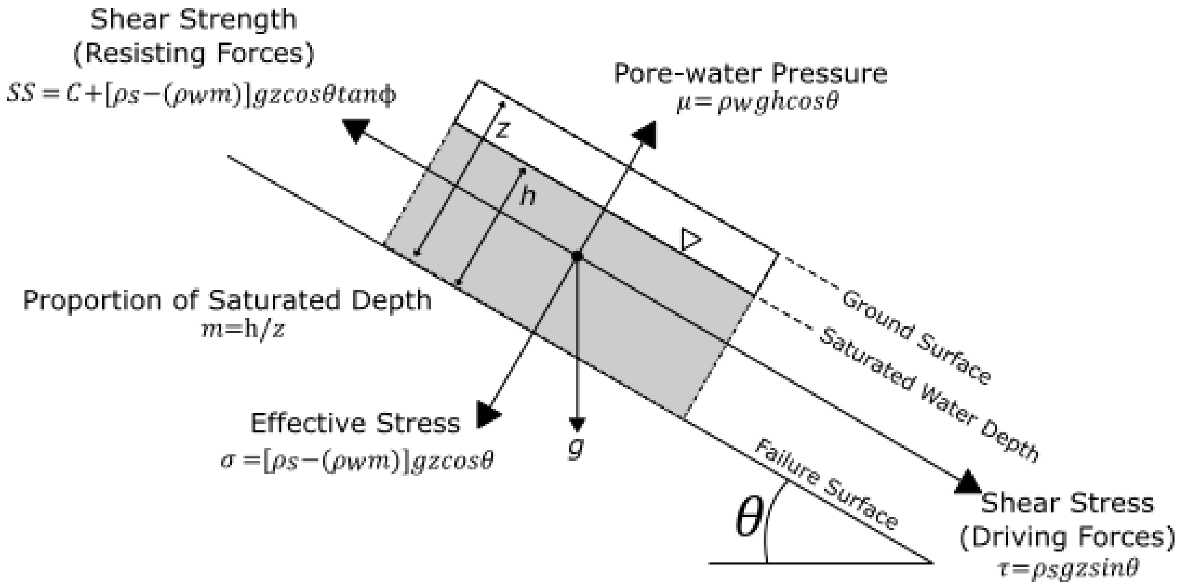

Figure 1.1: Block-diagram of landslide mechanics illustrates the importance of pore-water pressure in the force balance. Pore-water pressure $\boldsymbol{\mu}$ increases with saturated water depth $\boldsymbol{h}$ above the failure surface and reduces the effective stress $\boldsymbol{\sigma}$ acting on the failure plane. This effectively reduces the force of friction and cohesion, reducing the shear strength of the hillslope. Modified from Bierman and Montgomery (2013).

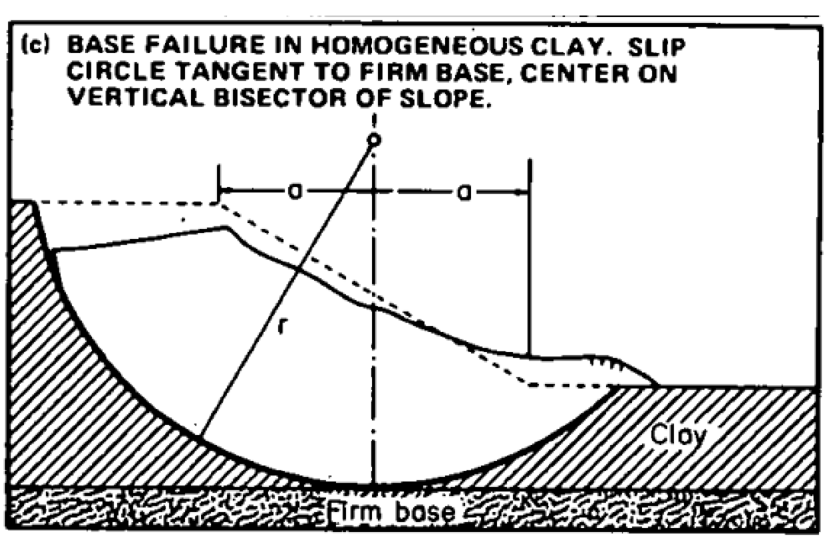

Figure 1.2: Rotational landslides are defined by the curved failure plane. They often develop blocks that rotate and move semi-independently. Each block moves relative to the center of rotation, causing some sections of the slide, such as the toe block, to move up, such as is seen with the Salmon Falls slide. Figure directly from (Varnes, 1978).

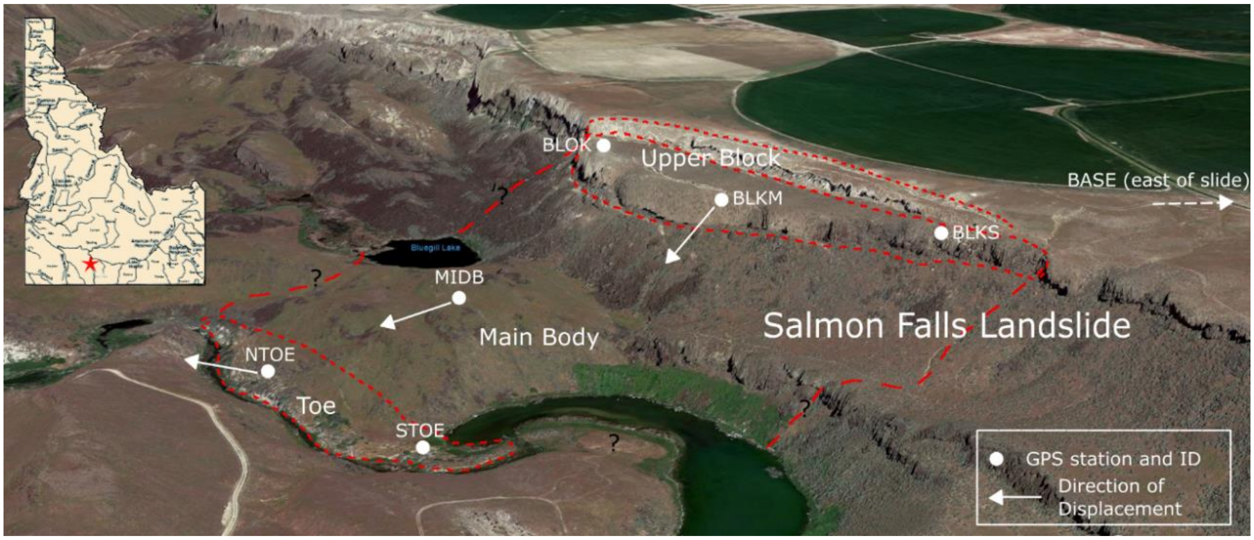

Figure 1.3: Salmon Falls landslide is located in central Idaho, along Salmon Falls Creek, 10 km west of Buhl, ID. It has three distinct kinematic domains: the upper block, middle, and toe. Additionally, three distinct water features are visible here, Salmon Falls Creek, Bluegill Lake, and the canal above the canyon rim.

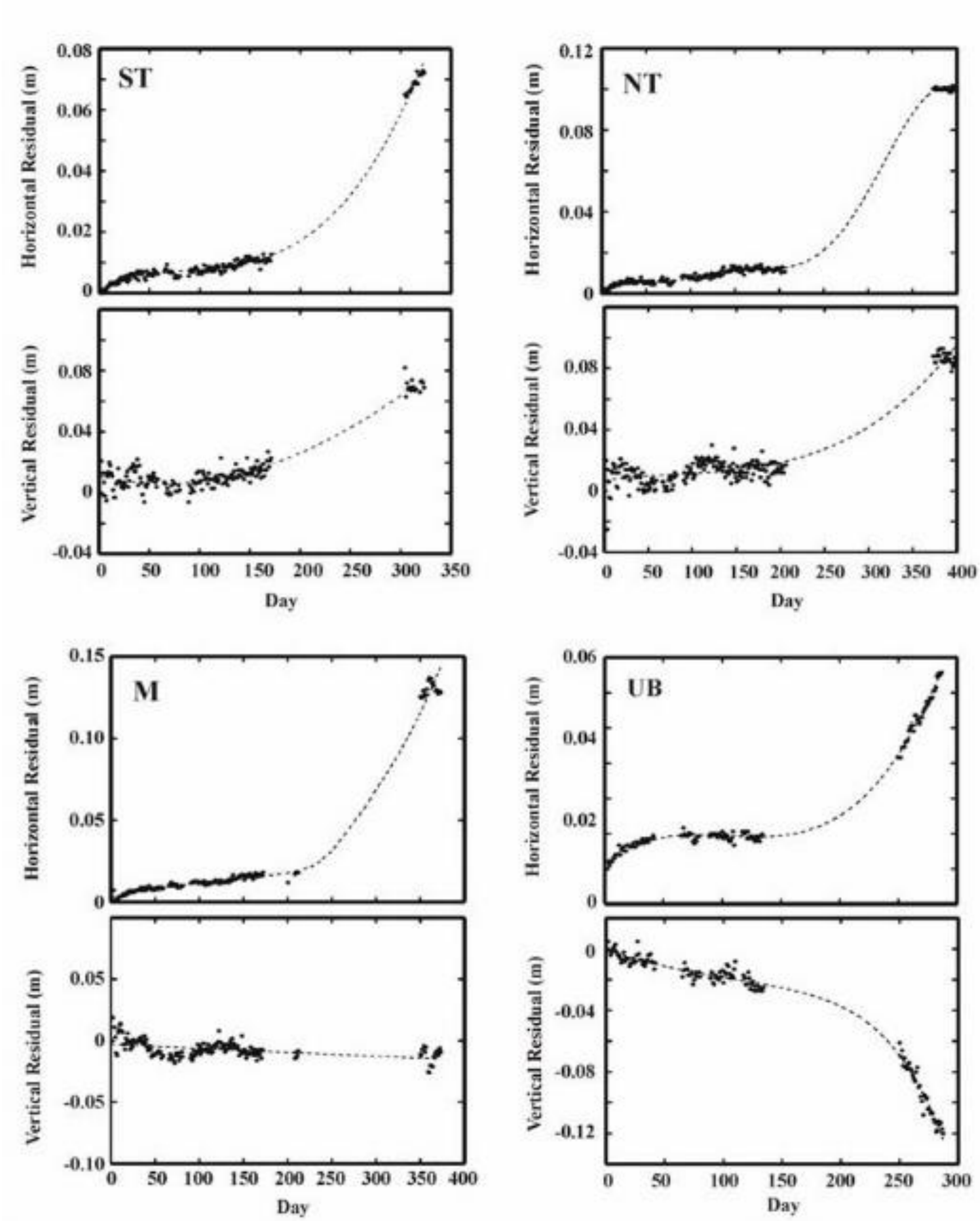

Figure 1.4: Figure directly from Dorsch (2004), Figure 19. GPS time series of the four original stations utilized by ISU in the 2003 survey. Day zero is February 20, 2003. Note the large interpolated period with the dashed line. Stations correspond with the following modern station names and location: ST = STOE (South Toe), NT = NTOE (North Toe), M = MIDB (Middle), UB = BLOK (Upper Block, north).

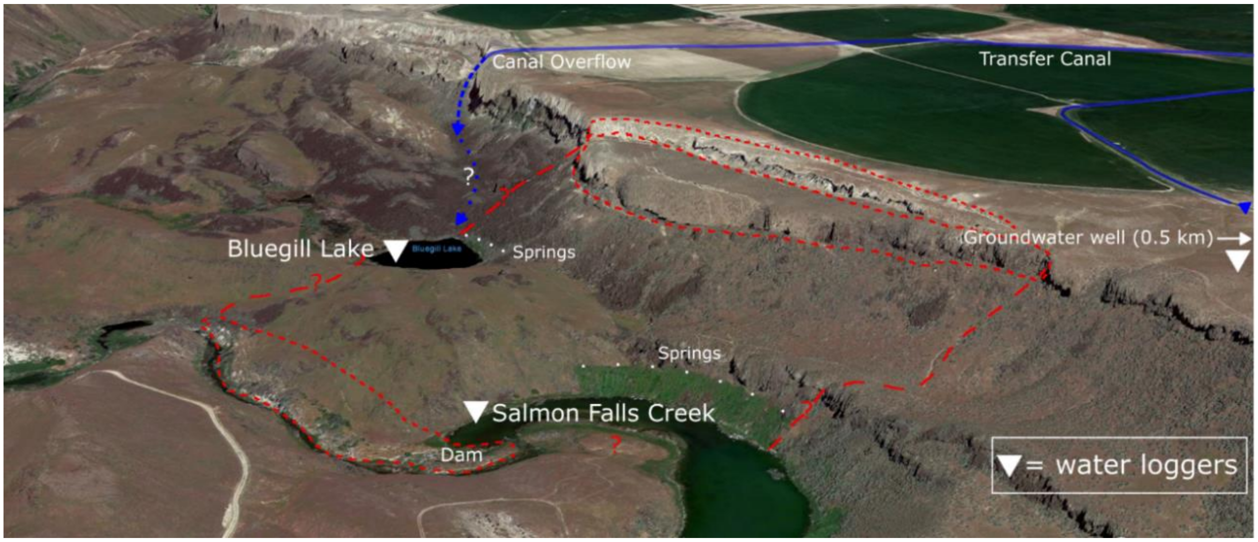

Figure 1.5: The study area has several important water features that contribute to a complex hydrogeologic system. Timing, volume, and spatial relationships between these various water sources and sinks are analyzed for landslide interaction. Not shown here, precipitation contributes both immediately to the study area and also to fluctuations in depth at Salmon Falls Creek, whose drainage area is south of the slide.

Chapter 2: Assessing the influence of water sources on slump movement

2.1 Abstract

Long-term monitoring and analysis of landslide drivers is a critical component to understanding how and when landslide hazards will occur and how to best mitigate them. Previous observation of the Salmon Falls landslide, a deep-seated, slow-moving, rotational slump, recorded accelerated movement during the dry summer months, conflicting with the expected behavior of landslides and water. These researchers hypothesized that anthropogenic water supply might be the cause, but the study lacked any hydrogeologic data to further support the relationship. In this study, we monitor the motion of the Salmon Falls landslide and potential drivers of landslide activity including fluctuations in multiple local water sources, a known driver of landslide motion. Coordinated observations from high-precision GPS and piezometers reveal that landslide velocity is highly sensitive to changes in local groundwater depth. The slump actively moves throughout much of the year, and this movement is marked by several prominent periods of acceleration and deceleration. These accelerations correlate to fluctuation in water depth at Bluegill Lake, a back-rotated depression on the body of the landslide fed by seasonal inputs from irrigation canals and precipitation. Landslide velocity varied by a factor of 10, from 0.1 to 1 mm/day, with an estimated change in water depth of 1.2 m. These findings support the expected relation between groundwater depth and landslide motion and highlight the significance of anthropogenic water sources as a potential contributor to landslide activity in the area.

2.2 Introduction

2.2.1 Motivation

Landslides are one of the most prevalent and costly geologic events around the world. The global effect of landslides and other mass-wasting events is estimated at 3.5 billion USD/yr (Singhroy et al., 2000; Danger, 2005) and results in the loss of approximately 1000 lives each year (Petley, 2012). Landslide are an important part of natural landscape evolution processes and are distributed in nearly all natural environments. This wide distribution creates high variability in landslide type, setting, and characteristics. Therefore, site-specific or localized studies are often necessary to characterize feature behavior in a given environment. Understanding the conditions that control landslide initiation and subsequent movement is paramount to both predicting their occurrence and minimizing the associated hazards and risks to natural and human resources.

One of the most frequently researched environmental conditions driving landslide motion is water. It has been shown that both precipitation (Guzzetti et al., 2008) and groundwater levels (Coe et al., 2003; Vallet et al., 2015) are important factors in considering the mechanical stability of slopes. Failure or motion of hillslopes is typically associated with increased pore-water pressure decreasing the effective stress in a landslide. Landslide sensitivity to water sources depends on a variety of factors including material characteristics, depth of failure, slide geometry, and other features such as preferential flow paths (Van Asch et al., 1999). Landslides are shown to be sensitive to even small fluctuations in pore-pressure (Schulz et al., 2009) and have been shown to be susceptible to locally elevated water from anthropogenic sources, such as multiple failures at the Hagerman Fossil Beds, Idaho (Chleborad and Powers, 1996; Farmer, 2003)

and others in White Bluffs, Washington (Bareither et al., 2012; Schuster et al., 1989).

2.2.2 Impetus

The Salmon Falls landslide is an active slump in Idaho that has been identified by previous researchers as having episodic movements and potential for groundwater-driven behavior (Chadwick, Dorsch, et al., 2005; Dorsch, 2004). Knowledge of kinematics for deep-seated rotational slides and their controls are generally understudied (Gokceoglu and Sezer, 2009), but this is of significant value to land managers trying to predict landslide behavior and mitigate potential hazards (Danger, 2005). Salmon Falls has been a frequent test site for landslide work, including recent efforts focused on characterizing its kinematic behavior (Glenn et al., 2006; Necsoiu et al., 2014). However, little is known about what conditions influence the slide's movement and how this varies over time. Recent studies have shown that episodic movements often associated with deep failures are driven by pore-water pressure relationships (Preisig et al., 2016). Monitoring of pore-water pressure in deep-seated slides can be particularly problematic because placing sensors directly at or near the failure plane landslide can be exceedingly difficult due to the depth of placement and shearing motion of the slide. By taking advantage of readily available surface water features along with local, pre-existing wells, we hope to evaluate the impact of groundwater fluctuation on landslide activity without the need for more expensive direct measurements.

In this study, we monitor multiple potential drivers of landslide activity including three potential sources of groundwater depth and precipitation records. We first quantify landslide deformation through continuous GPS observation. Then we analyze the effect of water level on GPS-derived landslide velocity. With this data we pursue the following questions about the Salmon Falls Landslide.

1. How does landslide motion vary over time?
2. Does landslide velocity vary as a function of water level?
3. How do various water sources contribute to the overall change in water depth measured in the slide?

2.3 Setting

The Salmon Falls landslide is deep-seated, slow-moving, rotational slump located along Salmon Falls Creek, a tributary of the Snake River in southern Idaho. It is the youngest event in a history of mass-wasting in the canyon and lies 400m south of a larger slide that failed in 1937 (Lee, 1938; Dorsch, 2004). Once called the “Sinking Canyon” (Buhl Herald, 1937), the recent history of mass-wasting is evident, but this is only the continuation of pre-historic legacy of events, several of whose features have been reactivated and expanded by modern failures. Salmon Falls Creek is not unique in this regard, and landslides have been observed to be a common actor in canyon evolution regionally, such as in the deeply-incised river networks of the Snake River Plain and analogous regions in eastern Oregon and Washington (Ely et al., 2012; Safran et al., 2015).

Reactivation of the Salmon Falls landslide was first noticed in 1998 by rock climbers and initially studied in the early 2000s. The Salmon Falls slump failed along a section of the canyon rim and displaces this mass down and west into Salmon Falls Creek, encompassing a total active area of 0.25 km^2 (Figure 2.1). The landslide failed primarily in the unconsolidated fluvial and lacustrine sediments of the Glenns Ferry Formation (Dorsch, 2004), which are locally interbedded with and then capped by volcanic flows. The thickest basalt flows define the canyon rim and compose a relatively cohesive upper block of the slide, which is 0.5 km long by 0.1 km wide. The upper block is separated from the canyon rim by the active scarp, which is 18 m tall at its highest and decreases to the south where it ramps up to meet the canyon rim. Horizontal separation of the main block from the canyon rim has formed a deep fissure along the back of the block. The pre-historic main body of the slide along canyon floor is composed of multiple cohesive blocks of canyon rim basalt entrained within landslide deposits and sediment and back-tilted by continued rotation towards the failure plane. The failure plane is proposed to be very deep, estimated between 50-100m below the ground surface in the middle of the slide based on proposed slide block geometry (Necsoiu et al., 2014).

The landslide is composed of three major domains: the upper block, the middle, and the toe. These are defined by both topographic expression (Figure 2.1) and distinct kinematics. The upper block of the landslide is composed primarily of a thick package of relatively cohesive basalt flows deposited over an unconsolidated sedimentary package. The unconsolidated sediments are relatively confined by the scarp in the back and by a steepened debris and talus hillslope in the front (Figure 2.1). Behind the active head scarp of the upper block exist two relic scarps which have accommodated 3-5m of displacement historically, but appear stable at present (Ellis et al., 2004). The middle of the landslide is composed of several large, broken blocks of canyon rim basalt that are back tilted towards the failure plane and entrained within landslide debris and sediment (Figure 2.1). The toe of the landslide is a relatively thin deposit of the typical basalt and sediment debris with the addition of fine fluvial deposits associated with Salmon Falls Creek (Figure 2.1) (Dorsch, 2004). The toe is defined by its distinct upward throw that is likely associated with upward thrusting of the area over a ramp in the curved failure plane (Dorsch, 2004; Necsoiu et al., 2014). The displacement of the toe is partially responsible for the damming of Salmon Falls Creek (Ellis et al., 2004). Movement of the landslide has maintained the river profile at relative equilibrium between incision rates and uplift of the toe.

In addition to the landslide kinematics, local hydrology is an important factor in determining the causal behavior of the slide. Three major hydrologic systems are significant in this study: Salmon Falls Creek, the local water table east of the canyon, and irrigation infrastructure. Salmon Falls Creek drains a 5450 km^2 south of the slide, including watersheds along the border between Idaho and Nevada. Much of this water is held at the Salmon Falls reservoir 65km upstream of the landslide, which feeds both the creek and a large canal diversion. Streamflow is regulated by the reservoir and is additionally modified by water-rights withdrawal and the presence of 3 low-head dams between the reservoir and the slide. The creek is dammed at the southern toe of the slide (Figure 2.2) and retains an estimated 325,000 m^3 of water (Ellis et al., 2004). Additional water withdrawals occur downstream of the landslide and upstream of the USGS gaging station near the confluence with the Snake River (USGS 13108150).

The regional groundwater system is understudied, has little to no modern literature, which has mostly been the focus of exploration for hydrothermal resources (Lewis and Young, 1982, 1989). Studies suggest a productive regional water table at an elevation of 1066 m that exists in the Pleistocene aged sedimentary deposits, likely Glenns Ferry Formation (Figure 2.3) (Lewis and Young, 1989; Chleborad and Powers, 1996). The 1981 to 2010 average annual precipitation is 26.1 cm/yr, 17.8 cm/yr of which falls as snow (WRCC, 2010). Most precipitation accumulates from November to May, and conversely water withdrawal is greatest in the summer from June to September.

Previous work on the Salmon Falls landslide has focused on characterizing landslide domains, describing its kinematics, and assessing its potential hazards. BLM, USGS, and ISU researchers performed initial observation of the slide in the early 2000's, measuring deformation with a variety of sensors including extensometer, theodolite, and GPS, some of which remains unpublished but was mostly summarized in Dorsch, 2004. They concluded that early movement accommodated a total of 8m of displacement up to 2003 and that the landslide slowed around this time to an average of 10-15 cm/yr with a peak rates of 40 cm/yr (Chadwick, Dorsch, et al., 2005; Dorsch, 2004; Ellis et al., 2004). Early hazard assessment investigated the damming of Salmon Falls Creek at the toe, but found no immediate danger (Ellis et al., 2004). Several LiDAR surveys were completed in 2002, 2005, 2011 and utilized the slide for experimental work, an early testbed for LiDAR change detection and illustrating differences in surface roughness and fractal geometry between the 1937 and 1990 slides (Glenn et al., 2006). Most recently, an InSAR study confirmed slide geometry and refined cross-sectional interpretation of the slide (Necsoiu et al., 2014).

2.4 Previous Work and Impetus

Although Salmon Falls landslide has been well studied, it is still unknown what conditions regulate the landslide's motion and how these vary in space and time. Previous researchers noted variation in landslide motion on scales of months to years and proposed potential connections to groundwater fluctuation, a known driver of landslide activity, but did not possess sufficient data to investigate further (Chadwick, Dorsch, et al., 2005; Dorsch, 2004).

Additionally, although previous GPS and InSAR studies characterized the kinematic elements of the slide, they had insufficient temporal resolution to resolve long-term variation in behaviors. In a 2003 GPS survey, landslide motion was found to be highest in late summer to fall and coincided with the driest season in Idaho when precipitation and groundwater levels were expected to be at a minimum (Chadwick et al., 2005; Dorsch, 2004). This observation opposed the expected behavior of pore-water pressure driven landslide activity, which predicts increased sliding with increased groundwater depth above a failure surface. Therefore, researchers suggested the relationship may be complicated by additions of water from an unlined irrigation ditch which feeds agricultural land along the canyon rim and runs parallel to the slide (Dorsch, 2004).

To elucidate the previously unresolved connections to landslide motion, we utilized a network of continuously operating GPS stations and piezometers to observe landslide motion and local water levels. We then compare the fluctuations in water depth to landslide velocity for possible correlation and interpret the hydrogeologic connection between various water sources and landslide movement.

2.5 GPS Methods and Results

2.5.1 GPS Deployment

Seven high precision, continuously operating GPS stations were utilized in a semi-permanent network to observe landslide velocity from January 2017 to March 2018. All stations were installed on permanently fixed threaded rod anchored in bedrock, large stably-entrained boulders, or concrete pylons. All GPS stations utilized Topcon “black-box” campaign kits supplied by UNAVCO. Each station was composed of a Topcon GB-1000 receiver and APS-1 antenna and powered by a solar panel. Six stations were installed across the landslide body, spatially distributed to represent the slide's three major domains (Figure 2.1). These stations included the original four stations from the 2003 survey (Dorsch, 2004; Chadwick, et al., 2005) along with two new stations, BLKM and BLKS. The two new stations were established on the middle and southern sections of the upper block of the landslide to observe the motion of the upper block and to resolve if differential movement occurred across its length. A section of the upper block containing the original BLOK station had begun to separate from the main feature previous to this survey and was no longer representative of that domain. The seventh station, BASE, reoccupied a previously established monument 1.5km east of the landslide that was used as a stable reference point.

2.5.2 GPS Data and Processing

GPS observations produced a time-series of positions for each monument which were utilized for daily velocity estimates. GPS stations continuously observed station position at 1 Hz and recorded averaged position on 15 second epochs. Observations were collected monthly and delivered to UNAVCO for processing. Daily positions relative to the Stable North American Reference Frame (SNARF) were calculated for each site by GAGE/PBO automated processing at Central Washington University and New Mexico Institute of Mining and Technology (Herring et al., 2016). GAGE processing provides a clean, well-tested processing solution for continuous GPS observation with accuracies of <1-2 cm and sub-cm precision at well-established sites. Movement of the reference station, BASE, was subtracted from each position time-series to reduce the effect of tectonic plate motion and other anomalous, local signals from the slump's movement.

Position time-series were fitted with a non-parametric model and then used to calculate time-series of station velocities. Position time-series were fitted with a smoothing spline interpolation in MATLAB’s Curve Fitting Toolbox to both reduce inherent GPS noise in daily position estimates and to fill minor gaps in the data. Because previous observation showed patterns in landslide velocity that varied on scales of weeks to months, a smoothing parameter of 0.001 was chosen, which respected velocity trends over the period of 7-10 days and produced fits to original data with an average confidence greater than $r^2 = 0.98$ and average RMSE of 2.9 mm (Table 2.1). Smoothing models were produced for each station and GPS vector component individually. The three-dimensional daily displacement for each station was calculated from north, east, and up components and the vector azimuth was determined. Daily velocity estimates were calculated from the smoothed daily displacement time series and utilized for regression analysis.

2.5.3 GPS Results

GPS stations recorded movement on each domain of the landslide, revealing their kinematic relationships and temporal patterns of landslide movement. All movements were determined relative to reference station motion, which averaged 1-2 mm/yr to the west and was an order of magnitude smaller than movement observed on the landslide at ~20cm/yr. Therefore, the subtraction of the BASE signal from the landslide stations was minimal and had little significance in the rest of the products. Precision of daily positions ranged from 1-3.7 mm, which is typically twice as great in the vertical component than the horizontal.

Although all six GPS stations on the landslide were processed and analyzed identically, we choose three stations to use for comparison to groundwater levels and other drivers: BLKM, MIDB, and NTOE. These three stations represented each of the three slide domains and form a rough transect of the landslide body (Figure 2.1).

The upper block has accommodated the most displacement on the northern end and progressively less displacement towards the south. The upper block has several significant fissures, mostly parallel to the main scarp, which typically accommodate 10-30 cm displacement each. A 2000 m^2 section of the northern-most end of the upper block where the BLOK station is located has begun to detach from the main upper block mass and is failing down and to the north-west at 32 cm/yr (Table 2.2), anomalous to the expected due west motion of the main block. The bulk motion of the upper block is represented by the middle block station, BLKM, and is failing down and to the west at 22.9 ± cm/yr (Table 2.2, Figure 2.4). The southern end of the block shows the smallest mean displacement of 3cm/yr (Table 2.2) and is still partially attached to the canyon rim at is southernmost tip. The main body of the landslide exhibits a mostly translational movement with little vertical signal (Figure 2.4). The MIDB station recorded an average velocity of 20.7 cm/yr to the west (Table 2.2). The toe is measured at its northern and southern end, NTOE and STOE respectively, which exhibit similar long-term movement trends. STOE had an average 3D velocity of 17.7 cm/yr, and NTOE moved at an average of 20.3cm/yr (Table 2.2).

2.5.4 Spatial and Temporal Patterns in Movement

The landslide exhibited behavior consistent with the current proposed kinematic model (Necsoiu et al., 2014). GPS station displacements support the landslide behaving as a rotational slump with three primary domains: the upper block, the middle, and the toe. The total 3-dimensional vector displacement for each slide domain was similar and ranged from 0.5-0.6

cm/day, or 18-22 cm/yr (Table 2.2), except for BLOK and BLKS which exhibit anomalous behavior explained previously. However, each station exhibited different partitioning of the total displacement between horizontal and vertical components. All stations move in a similar west-southwest direction but with differing vertical displacement as shown in Figure 2.4. The upper block (BLOK) moves down, the toe (NTOE) moves up, and the middle (MIDB) moves mostly horizontal with little vertical change.

Time-series of velocity indicate that all three slide domains move almost continuously and simultaneously with minor deviations away from the overall trend (Figure 2.5). The slide was previously considered continuously active, however, from mid-February to April 2018 landslide velocity decreased below the limit for several weeklong periods. In general, long term trends in velocity are most visible in the horizontal component relative to vertical, and vertical velocity contributes a large proportion of the variability in the total three-dimensional vector velocity shown in Figure 2.6.

The GPS stations recorded three major acceleration events during deployment in 2017 and the beginning of a fourth in 2018. The first event reached maximum velocity of 0.6 mm/day (22 cm/yr) by mid-February, followed by a second peak of (36 cm/yr) in early June, and the third peak of 0.9 mm/day (33 cm/yr) by late October (Figure 2.6). The two largest acceleration events, which peaked in June and October 2017, occurred over a period of four to five months, while the smallest event occurred within a two-month cycle.

2.6 Hydrologic Methods and Results

Salmon Falls landslide has a complex water system, a result of high relief, multiple inputs, and complex morphology. Multiple water features are visible across the study area including creeks, lakes, dams, springs, and irrigation canals (Figure 2.1). To assess the potential contribution of these various water sources to the landslide, we used a combination of methods including water loggers, salt-dilution conductivity gauging, and field observations combined with historical datasets on stream activity, precipitation, and temperature.

2.6.1 Hydrologic Monitoring Methods

Water depth was measured at three locations along a transect of the landslide with Hobo U20 piezometric water level loggers. These locations represented the potential upper and lower limit of the groundwater system and one potential indicator of saturated water depth within the slide body (Figure 2.2). The natural water table above the canyon rim was inferred from elevation of the water surface measured in a well, 0.5km SE from the slide. The lower limit of the water system was inferred from the water level of Salmon Falls Creek just above the dammed section south of the slide toe. Finally, the potential saturated groundwater depth on the landslides body was measured at Bluegill Lake, which is perched on the middle section of the slide. Sensors were placed in perforated pipes anchored in the water features and suspended above the bed to prevent fouling of the instruments. Pressure and temperature were recorded every 15 minutes, barometrically compensated in the native HOBOWARE software, and then averaged daily to yield time-series of relative water depth, or stage, at each location. Daily time-series of water depth were then compared to other records including hydrographs from USGS gauge at Salmon Falls Creek (USGS 13108150) and historical well logs (U.S. Geological Survey, 2018).

In addition, canal discharge and water loss, precipitation, and temperature were analyzed for relationships both to fluctuation in groundwater levels and to movement of the slide. Discharge was measured at two locations along the reach of the canal immediately adjacent to the slide using salt dilution conductivity gauging (Payn et al., 2009). Discharges from the two sites were differenced to reveal water loss per length distance along unlined canal. Weather records of temperature and precipitation were obtained from station the NOAA station in Castleford (USC00101551), 7 km east of the slide (NOAA, 2018).

2.6.2 Hydrologic Monitoring Results

2.6.2.1 Salmon Falls Creek

Salmon Falls Creek was monitored at two locations, in the dammed section adjacent to the landslide body and 11km downstream of the slide at a USGS gauging near the confluence with the Snake River (U.S. Geological Survey, 2018). The two locations exhibited high similarity despite several modifications to the creek between sites (Figure 2.7) including a pumping station and low head dam downstream of the landslide. Baseflow is regulated by the Salmon Falls Creek dam 64.5 km upstream of the landslide but is highly modified both by water rights withdrawal and inputs from several large drainages downstream of the dam. We found that water levels fluctuate often on Salmon Falls Creek but are organized into four seasonal periods, shown in Figure 2.7. Moderate stage is exhibited during winter from November to April and is followed by spiked increases during spring precipitation or dam releases. After spring, flows decrease dramatically to yearly lows from June to September and are followed by a second period of increased peak flow from September to October. Flows then progressively drop back to winter levels.

During February 2017 and coinciding with our study, an anomalous, extreme rain-on-snow event caused significant flooding in the area. In Salmon Falls creek, discharge surged from its winter value of 4 m^3s^{-1} to over 20 m^3s^{-1}, over 5 times the normal discharge (February 2017

Figure 2.8). Again, in mid-May a spike in discharge of 14 m^3s^{-1} is seen, which is associated with a large water release from the dam (May, Figure 2.8). These two high discharge events produced visible channel incision, and knickzones were observed migrating rapidly upstream in the reach below the dam and adjacent to the toe of the slump. The streambank opposite and downstream of the landslide dam was cut back approximately one meter and produced multiple bank failures during February 2017.

2.6.2.2 Bluegill Lake

Bluegill Lake is a body of water elevated mid slope of the Bluegill landslide in a depression on its northern boundary (Figure 2.2). Its surface is elevated approximately 15m above water level at Salmon Falls Creek and 60m below groundwater tables at the well, shown in Figure 2.3. It has no surficial inlet but does have occasionally overflow via an outlet to Salmon Falls Creek north of the slump area (Figure 2.2). Water is present in Bluegill Lake year-round with a punctuated increase in water level from early April through late October, as shown in Figure 2.7. In the second week of April, coinciding with beginning of irrigation water flow in the canal, water levels in the lake rise from 1m relative depth to 2.25 m meters. As water levels near 2.2 m depth, the outlet channel is breached, and water begins to flow from Bluegill Lake to Salmon Falls Creek. The outlet height appears to control the maximum water depth in the lake during the summer at 2-2.25 m depth. Summer high water is interrupted by two short periods of decreasing stage in early July and again in early August. Water levels remain relatively high until the last week of October, coinciding with irrigation canal shutoff on October 30th (Salmon River Canal Co. 2018, pers.comm., 13 February), and then drop steadily through winter and into spring. Levels rise abruptly again in late April 2018 coinciding with initiation of flow in the irrigation canal.

2.6.2.3 Groundwater Level at Well Site

Local groundwater level measured at the well exhibits an annual cycle of water gain and loss with an amplitude of ~2 meters and little inter-annual variability (Figure 2.7). Yearly average elevation of the water table is of 1063m, which correlates well with modelled estimates of 1065m (Lewis and Young, 1989). Because we are interested in fluctuation in groundwater depth, water levels are reported relative to the depth of the water logger. Throughout the spring and into May, relative water level is stable at 6.6 ± 0.05 m. In the first week of May, water levels begin to drop steadily, coinciding with water withdrawal from the well, whose drawdown is recorded infrequently 2-3 time per week. Local drawdown from pumping draws water levels down by ~1.5m and typically last 2-3 hours before recovery back to static water level. These brief events were removed from our plotted time series. Water levels continue to drop until the first week of August when it stabilizes at an average water level of 5.7m. Beginning in the first week of September, water levels begin to steadily gain again until reaching a maximum of 7.5 m in early November. From November through May 2018, water levels steadily decline and then decline more rapidly once regional irritation pumping begins again.

2.6.2.4 Irrigation Canal

An unlined irrigation canal runs along the canyon rim east of the landslide headwall, providing water for agricultural use. Unused water from the canal overflows the canyon rim 450 m north of the slide area and into a talus field sloping down toward the slide (Figure 2.2). Water flows in the irrigation canal annually from mid-April until late-October and was confirmed to be turned on April 10-14th and off on October 30th for the study period in 2017 (Salmon River Canal Co. 2018, pers.comm., 13 February). Salt dilution gauging on October 18th, 2017 yielded a discharge of 23.2 L/sec on the upper end of the reach and 22.5 L/sec 0.66 km downstream. This channel reach is immediately parallel to the scarp of the slide and has a calculated loss of 3%, or -17.8 m^3/day. Based on a 3% per length loss, we estimated a total volume of 45,000 m^3/yr lost over the 2.5km reach adjacent to the slide in a total active period of 200 days. The remaining discharge at the end of the canal is estimated to be 21 L/sec, which overflows the canyon rim directly into the drainage above Bluegill Lake. A total volume of 366,000 m^3 of water is estimated to overflow the canyon rim during its active season. This estimation does not account for water withdrawal along the stretch of canal, which likely reduces these estimates significantly during months of heavy irrigation in July and August. Nonetheless, the entire unused proportion of water in the irrigation canal either overflows the canyon rim or infiltrates the unlined canal structure adjacent to the slide.

2.6.2.5 Precipitation and Weather

Precipitation and temperature data collected from NOAA station USC00101551, 8 km south of the slide, were utilized to supplement water level collections (Figure 2.7). Importantly, heavy mid-winter rains are recorded in February 2017 and resulted in a rain-on-snow event in the region that produced heavy flooding conditions recorded in Salmon Falls Creek (Figure 2.8). Precipitation accumulates the most during spring months from February to April and then is relatively absent and dry until the beginning of fall storms occurring from September to November.

2.7 Interpretation: Influence of Hydrology on Landslide Behavior

2.7.1 Landslide Kinematics

Salmon Falls landslide was found to move near continuously and exhibited three distinct periods of acceleration within the year of observation. Magnitude and timing of accelerations are similar across the landslide, with the exception of the upper block, whose middle station is most representative of the bulk movement. The upper block has clear differential movement that progresses from the smallest at the southern end, BLKS, to the largest at the northern end, BLOK. Direction of displacement on each of the landslide domains continues to support the interpretation of a rotational failure.

Patterns of acceleration differed from those found in the 2003 survey but exhibited similar average velocity. The 2003 survey recorded only a single 200+ day acceleration that displaced the slide ~12cm over ~200 days at an average velocity of 0.6 mm/day. The 2017 survey recorded three accelerations with a total displacement of 9.7cm and 8.1cm in the summer and fall accelerations respectively, occurring over approximately 120 days each, and had an average velocity of 0.8 mm/day and 0.7 mm/day. Importantly, the 2003 survey occurred during a period of drought and is contrasted by the heavy precipitation and flooding which occurred during the 2017 survey. Assuming connections between landslide velocity and water, the lack of precipitation and a potential for greater water withdrawal from the irrigation system during the 2003 period may have resulted in significantly lower contribution of water to the slide and differences in observed landslide behavior between the two surveys. Particularly, the spring to early summer of 2017 was very wet, likely leading to less irrigation consumption by sprinklers and more water overflowing into the landslide, whereas in 2003 irrigation withdrawal may have begun earlier and at greater volume reducing inputs to the slide and producing only the single, fall acceleration.

In the spring 2018, slide velocities remain close to zero and below the limit to detect change for approximately two and a half months. Deviations away from a zero velocity during this period are difficult to interpret due to missing data but may represent brief, small adjustments in position. The increase in slide movement in 2018 appears to initiate prior to the initiation of irrigation in April 2018. That said, this timing is based largely on interpolated GPS positions because there is missing data at two stations during this time.

2.7.2 Water Level Patterns and Timing Overview

The hydrogeologic story at Salmon Falls landslide is complicated by multiple water sources and complex geology; however, several patterns were immediately apparent. First, groundwater depth above the landslide exhibited purely annual cyclicity, driven by seasonal precipitation and snow melt in the spring and irrigation consumption in the summer (Figure 2.7). Second, water depth in Salmon Falls Creek was similarly seasonal and punctuated with dam release or precipitation events, but its base flow was likely controlled mostly by the Salmon Falls dam, ~65 km upstream. Extreme precipitation events, such as the February 2017 flooding, were apparent in Salmon Falls Creek records and lead to a peak discharge of 3 times the normal peak flow during early spring (Figure 2.8). Third, water level trends in Bluegill Lake opposed those in the creek and well. Bluegill Lake gained depth in the summer, and lost in the winter, indicating that irrigation water is the likeliest drivers of variation in water depth at Bluegill Lake (Figure 2.7).

2.7.3 Analysis of Water Influence on Landslide Velocity

We independently compared time series of water depth, precipitation, and irrigation against landslide velocity measurements (Figures 2.9 to Figure 2.12). Strong correlations to landslide velocity would indicate potential coupling of the water source to saturated water depth within the slide body, and subsequent interaction with the failure surface.

Water levels at the well and Salmon Falls Creek, interpreted to represent the maximum and minimum groundwater elevation, show little similarity to patterns of slide movement. Water level within the well, the groundwater table east of the slide, showed a distinct lack of correlation to landslide velocity. The water table fluctuates with annual cyclicity, but landslide velocity fluctuates three times per year (Figure 2.9). From June to November, well water depths fluctuate in phase with velocity, but are dyssynchronous the rest of the year. Salmon Falls Creek fluctuates seasonally, with two periods of high stage separate by two periods of low stage, shown in Figure 2.10. Periods of high stage initially appear to occur in the early periods of landslide acceleration, but closer inspection reveals that landslide movement initiates before stage increases, discrediting stage as a driver for motion. Additionally, the magnitude and duration of landslide accelerations is not commensurate with changes in water depth at the creek.

Bluegill Lake shows immediate visual similarity to patterns in slide velocity, shown in Figure 2.11. Timing and magnitude of changes in water depth are commensurate with and slightly proceed changes in landslide velocity, indicating water depth at the lake may be associated in some way to groundwater depths driving slide motion. Correlation scatter plot of water depth vs velocity, Figure 2.13, shows a moderate, positive relationship but is confounded by a high variation in slide velocity at higher water depths. Grouping of points at high water depth appears to be caused by continued fluctuation of landslide velocity after Bluegill Lake has reached its maximum capacity at 2.2 m. To a smaller degree, correlation at low velocities and high-water depth appear to be decoupled, (Figure 2.13). This decoupling may be associated with the time-lag between water level change and subsequent reaction of the landslide. This is likely due to complexities in paths from water input to changes in depth at Bluegill Lake and then subsequent changes in saturated groundwater depth above the failure surface.

The accumulated precipitation record initially shows several interesting similarities to landslide velocity but is not convincing as a primary cause of acceleration (Figure 2.11). However, it is important to point out that one-third of the total yearly precipitation occurred in a two-week period during the middle of February and was associated with an intense rain-on-snow event that caused severe flooding regionally and appeared in the Salmon Falls Creek hydrograph (Figure 2.8). This flooding likely raised groundwater levels throughout the area and resulted in the following February acceleration event (Figure 2.12). Therefore, precipitation does have some effect on slide velocity, but may only be significant for high magnitude events relative to the influence of other drivers.

2.7.4 Bluegill Lake and Connections to Landslide Hydrogeology

Association between Bluegill Lake water levels and landslide velocity has been shown (Figure 2.8 and Figure 2.13), but the relationship between water level drivers, surficial water levels measured at the lake, and saturated water depth controlling velocity in the slide is still unclear. First, we propose that fluctuation in water level at Bluegill Lake is primarily driven by water introduced from the irrigation canal. Timing of irrigation correlates directly to rises in water level at Bluegill Lake in 2017 and 2018. However, there are two potential paths of water to the landslide, infiltration from the canal and direct discharge of excess irrigation water over the canyon rim. There is little to no lag between the onset of irrigation and water depth change at the lake, requiring that the subsurface flowpath have high transmissivity. This is unlikely because infiltrating water from the irrigation canal would have to travel through several hundred meters of sedimentary deposits with low vertical transmissivity and relatively high horizontal transmissivity along paleo-channels. This pathway is likely much slower still than direct discharge of water from the canal into the canyon by the irrigation overflow, which enters the slide area 450m north of the lake and would travel over the surface, through broken talus deposits downslope to the lake. Additionally, discharge measurements from the canal suggested 366,000 m^3 of water overflows the canyon rim during its active period compared to 45,000 m^3 which infiltrates from the canal in the same time. Therefore, it is most likely that the primary contribution of water to Bluegill Lake is irrigation canal water that overflows the canyon rim and follows a relatively quick path through broken talus to the Bluegill Lake area (Figure 2.14).

Two potential associations between lake level and groundwater depth are proposed: (1) Bluegill Lake is a perched water body fed by irrigation water which then infiltrates down to the local groundwater table, or (2) Bluegill Lake is the surficial expression of saturated water depth within the slide and locally elevates or mounds the water table proximal to the lake with additions of irrigation water. Springs occasionally emerge from the talus slope adjacent to and immediately above the lake at an elevation of ~1006m, and south of the slide at elevations of ~1001m, shown in Figure 2.2. The elevations of the springs suggest that a laterally continuous saturated water depth likely persists from Bluegill Lake across the middle body of the slide and to the southern springs. This connection may be due to preferential flow along the back tilted basalt blocks, which are oriented north-south in direction of potential flow and create the depression in which Bluegill Lake forms, shown in Figure 2.3. These blocks might potentially create the confinement upon which Bluegill and the rest of the water is perched, but these areas would be expected to exhibit high vertical transmissivity given the highly fractured and broken nature of the deposits. If Bluegill Lake was perched and controlled by seasonal water inputs, then water levels in the lake would be expected to recede rapidly until the lake was dry once the irrigation canal was turned off. However, Bluegill's water levels drop at a slow, steady rate after irrigation water is turned off, as shown in Figure 2.7, and the lake continues to persist through the winter until the next season. Therefore, the most likely answer is that saturated groundwater depth within the slide is relatively high year-round and is responsible for the persistence of Bluegill Lake.

2.7.5 Proposed Hydrogeologic Model

The behavior of Salmon Falls landslide appears to be controlled by a complex hydrogeologic system driven by seasonal fluctuations in groundwater availability, which are controlled primarily by overflow from an irrigation canal along the canyon rim. We propose a conceptual model where the saturated water depth in the landslide is determined by two fundamental stages (Figure 2.15). In the first stage, when irrigation water is absent in the fall through spring, saturated groundwater levels within the slide are at a minimum and are controlled by the natural water table. This follows the natural gradient between water tables measured at the canyon rim well and in Salmon Falls Creek at the base of the landslide (Figure 2.14). The minimum saturated depth on the slide is revealed by the year-round persistence of water within Bluegill Lake, which has no surficial inputs and does not occupy its outlet channel at low levels. In our survey, this occurred from November 2017 through April 2018.

In the second stage of the model, irrigation elevates the groundwater table in the slide body proximal to its input near Bluegill Lake and results in increased slide motion. Irrigation water is introduced in early spring (April 14th in 2017 and April 25th in 2018) to the canal along the canyon rim (Figure 2.14, 1) and any unused water is directed over the canyon rim into a talus field immediately north of the slide and Bluegill Lake (Figure 2.14, 2). This water flows through the talus slope to the depression in the landslide body containing Bluegill Lake. This water infiltrates the slide body proximal to the lake and elevates the local groundwater table (Figure

2.14, 3). Water continues to rise in Bluegill Lake as saturated water levels increase in the landslide until the lake exceeds the height of its outlet channel (Figure 2.14, 4). After Bluegill has reached its maximum capacity, irrigation water continues to be delivered to the slide and potentially raises saturated depth beyond levels expressed at Bluegill Lake, as evidenced by the presence of springs adjacent to the lake and on the south side of the slide (Figure 2.15, 4). During summer irrigation season, fluctuations in levels at Bluegill Lake are likely caused both by continued drop in regional groundwater levels, such as measured at the well, and from fluctuations the irrigation overflow, which is influenced by the amount of agricultural consumption along the canal.

2.8 Implications

In this study, we evaluate if known drivers of landslide activity are responsible for variation in landslide velocity as previously observed in the 2003 survey (Chadwick, Dorsch, et al., 2005; Dorsch, 2004) and whether kinematic behavior of the slide was still consistent with characterization of a deep-seated, rotational slump (Necsoiu et al., 2014). We found that landslide movement was not continuous and that its active period was punctuated by three accelerations in 2017. These findings were inconsistent with the continuous movement and single acceleration documented in the 2003 survey (Figure 2.18), but differences in survey observations may be attributed to significantly different hydrologic conditions, which contrast a persistent drought in 2003 against high precipitation and flooding in 2017. Our results show that deep-seated, slow-moving, rotational slumps follow the expected pore-water pressure driven behavior for landslides (e.g. Schulz et al., 2009), based on correlation between observations made at Bluegill Lake and landslide velocity. Additionally, we find these slides can be sensitive to small fluctuations in saturated water depth. Landslide velocity varied by a factor of 10, from 0.1 to 1 mm/day, with an estimated change in water depth of 1.2 m.

Prominently, we found that surficial water levels appear to be good indicator of saturated groundwater depth and correlated moderately well with changes in landslide activity. However, we required a two-part model to explain this behavior, because the sensitivity of our measurements at Bluegill Lake were limited by the lakes maximum capacity. We found that surficial water levels on the landslide were driven by seasonal availability of irrigation water, which was supplied to the landslide via surface and subsurface pathways. Because of these relationships, we could roughly estimate water contribution to landslide velocity without the need for more elaborate setups to directly measure pore-water pressure at the failure surface.

Irrigation water has been shown to be an important factor in factor in the redistribution of water in the natural environment. Our findings show locally elevated water levels could be caused by irrigation water loss and that volumetric water loss was reasonably sufficient to raise water depth to the height observed at Bluegill Lake. This confirms the potential for anthropogenic water drivers on landslide activity, which have been proposed by other studies (Chleborad and Powers, 1996; Farmer, 2003; Bareither et al., 2012). Irrigation systems are broadly used in the Snake River Plain, one of the areas in the nation with highest percentage of water withdrawal for agricultural use (Maupin et al., 2010). Redistribution of natural water supplies to the surface can cause new or elevated water tables and may have adverse effects on a variety of natural and built resources. Canal water loss measured adjacent to the slide was low at 3%, yet still contributed a significant volume of water to the area by directly channeling excess water over the canyon rim. Managers of these systems can utilize this knowledge to assess the potential impact of their systems and inform decisions to manage water distribution and engineer these systems. In this case, if stabilization of the slide became a priority, managers would be prudent in first redirecting the irrigation overflow by piping or other means, in order to reduce the total volume of water introduced to the system by greater than 80%, thus reducing landslide motion.

2.9 Conclusion

This study demonstrates the importance of anthropogenic modification on our natural environment, particularly how redistribution of water on the surface can significantly modify local groundwater systems and subsequently alter force balances in these natural systems. Hillslopes are particularly susceptible to these alterations and are of particular concern when evaluating how to build and maintain distribution networks for our water resources. These water distribution systems are an integral part of the economic resources available for many regions, so careful evaluation of their impact is a necessity to maintaining these valuable resources (Schuster et al., 1989; Farmer, 2003; Pereira et al., 2002).

Deep-seated, slow-moving, rotational slumps have been found to be susceptible to relatively small alterations in groundwater depth, confirming observations of previous researchers. We found surficial water bodies to be an effective estimate of groundwater fluctuations on this slide and found a positive, linear relationship between lake stage and landslide velocity. Indirect observation of groundwater depth expands the possibility for assessing these interactions in future landslides where direct sampling is impractical.

References

Van Asch, T.W.J., Buma, J., and Van Beek, L.P.H., 1999, A view on some hydrological triggering systems in landslides: Geomorphology, v. 30, p. 25–32, doi: 10.1016/S0169-555X(99)00042-2.

Bareither, C.A., Edil, T.B., and Benson, C.H., 2012, Investigation of White Bluffs Landslides in Washington State: GeoCongress 2012: State of the Art and Practice in Geotechnical Engineering, 2012, p. 546–555, doi: 10.1061/9780784412121.057

Buhl Herald, 1937, Earth sinking into underground cave : Buhl Herald, Buhl, Idaho

Chadwick, D.J., Dorsch, S.J., Glenn, N.F., Thackray, G.D., and Shilling, K., 2005, Application of multi-temporal high-resolution imagery and GPS in a study of the motion of a canyon rim landslide: Photogrametry and Remote Sensing, v. 59, p. 212–221, doi: 10.1016/j.isprsjprs.2005.02.001.

Chadwick, D.J., Thackray, G.D., and Glenn, N.F., 2005, Landslide Surveillance : New Tools for an Old Problem: Eos, Transactions American Geophysical Union, v. 86, p. 109–120, doi: 10.1029/2005EO110001

Chleborad, A.F., and Powers, P.S., 1996, Slope map and locations of irrigation-induced landslides and seepage areas, Hagerman Fossil Beds National Monument, Idaho: U.S. Geological Survey Open-File Report 96-258, 1 p., http://pubs.er.usgs.gov/publication/ofr96258.

Coe, J.A., Ellis, W.L., Godt, J.W., Savage, W.Z., Savage, J.E., Michael, J.A., Kibler, J.D., Powers, P.S., Lidke, D.J., and Debray, S., 2003, Seasonal movement of the Slumgullion landslide determined from Global Positioning System surveys and field instrumentation, July 1998 – March 2002: Engineering Geology, v. 68, p. 67–101, doi: 10.1016/S0013-7952(02)00199-0.

Danger, A.N., 2005, Landslide Hazards — A National Threat, Landslide potential of the conterminous United States: U.S. Geological Survey Fact Sheet 2005-3156, 2 p. https://pubs.usgs.gov/fs/2005/3156/2005-3156.pdf.

Dorsch, S.J., 2004, The Geologic framework, movement history and mechanics of the Salmon Falls Landslide, Twin Falls County, Idaho [M.S. thesis]: Idaho State University, 138 p.

Ellis, W.L., Schuster, R.L., and Schulz, W.H., 2004, Assessment of hazards associated with the Bluegill Landslide, South-Central Idaho: U.S. Geological Survey Open-File Report 2004-1054. 16 p.

Ely, L.L., et al., 2012, Owyhee River intracanyon lava flows: Does the river give a dam? Geological Society of America Bulletin, v. 124, p. 1667–1687, d oi: 10.1130/B30574.1

Farmer, N., 2003, Hagerman Valley landslides triggered by land-use change endanger lives, and destroy natural and cultural resources (Hagerman Valley Fossil Beds National Monument, NPS, Idaho): Journal of the Japan Landslide Society, v. 40, p. 341–343, doi: 10.3313/jls.40.4_341.

Glenn, N.F., Streutker, D.R., Chadwick, D.J., Thackray, G.D., and Dorsch, S.J., 2006, Analysis of LiDAR-derived topographic information for characterizing and differentiating landslide morphology and activity: Geomorphology, v. 73, p. 131–148, doi: 10.1016/j.geomorph.2005.07.006.

Gokceoglu, C., and Sezer, E., 2009, A statistical assessment on international landslide literature (1945-2008): Landslides, v. 6, p. 345–351, doi: 10.1007/s10346-009-0166-3.

Guzzetti, F., Peruccacci, S., Rossi, M., and Stark, C.P., 2008, The rainfall intensity-duration control of shallow landslides and debris flows: An update: Landslides, v. 5, p. 3–17, doi: 10.1007/s10346-007-0112-1.

Herring, T.A., Melbourne, T.I., Murray, M.H., Floyd, M.A., Szeliga, W.M., King, R.W., Phillips, D.A., Puskas, C.M., Santillan, M., and Wang, L., 2016, Plate Boundary Observatory and related networks: GPS data analysis methods and geodetic product: AGU Reviews of Geophysics, v. 54, i. 4, 50 p., doi: 10.1002/2016RG000529.

Lee, C.A., 1938, Recent Landslides in Salmon Creek Canyon, Idaho: The Journal of Geology, v. 46, p. 660–665, doi: 10.1086/624667

Lewis, R.E.E., and Young, H.W., 1982, Geothermal resources in the Banbury Hot Springs area, Twin Falls County, Idaho: U.S. Geological Survey Water Supply Paper 2186, v. 27, 32 p.

Lewis, R.E., and Young, H.W., 1989, The hydrothermal system in central Twin Falls County, Idaho: U.S. Geological Survey Water-Resources Investigation Report 88-4152, 44 p.

Maupin, M.A., Kenny, J.F., Hutson, S.S., Lovelace, J.K., Barber, N.L., and Linsey, K.S., 2010, Estimated Use of Water in the United States in 2010: U.S. Geological Survey Circular 1405, 64 p., doi: http://dx.doi.org/10.3133/cir1405.

Necsoiu, M., McGinnis, R.N., and Hooper, D.M., 2014, New insights on the Salmon Falls Creek Canyon landslide complex based on geomorphological analysis and multitemporal satellite InSAR techniques: Landslides, v. 11, p. 1141–1153, doi: 10.1007/s10346-014-0523-8.

National Ocean and Atmospheric Association, 2018, Castleford, ID Station Data Inventory: https://www.ncdc.noaa.gov/cdo-web/datasets/GHCND/stations/GHCND:USC00101551/detail.

Payn, R.A., Gooseff, M.N., McGlynn, B.L., Bencala, K.E., and Wondzell, S.M., 2009, Channel water balance and exchange with subsurface flow along a mountain headwater stream in Montana, United States: U.S. Geological Survey Water Resources Research, v. 45, 14 p., doi: 10.1029/2008WR007644.

Pereira, L.S., Oweis, T., and Zairi, A., 2002, Irrigation management under water scarcity: Agricultural Water Management, v. 57, i. 3, p. 175–206, doi: 10.1016/S0378-3774(02)00075-6.

Petley, D., 2012, Global patterns of loss of life from landslides: Geology, v. 40, p. 927–930, http://dx.doi.org/10.1130/G33217.1.

Preisig, G., Eberhardt, E., Smithyman, M., Preh, A., and Bonzanigo, L., 2016, Hydromechanical rock mass fatigue in deep-seated landslides accompanying seasonal variations in pore pressures: Rock Mechanics and Rock Engineering, v. 49, i. 6, p. 2333–2351, doi: 10.1007/s00603-016-0912-5

Safran, E.B., O'Connor, J.E., Ely, L.L., House, P.K., Grant, G.E., Harrity, K., Croall, K., and Jones, E., 2015, Plugs or flood-makers? the unstable landslide dams of eastern Oregon: Geomorphology, v. 248, p. 237–251, doi: 10.1016/j.geomorph.2015.06.040.

Schulz, W.H., McKenna, J.P., Kibler, J.D., and Biavati, G., 2009, Relations between hydrology and velocity of a continuously moving landslide-evidence of pore-pressure feedback regulating landslide motion: Landslides, v. 6, p. 181–190, doi: 10.1007/s10346-009-0157-4.

Schuster, R.L., Chleborad, A.F., and Hays, W.H., 1989, The White Bluffs landslides: Engineering Geology in Washington, Washington Division Geology and Earth Resources Bulletin 78, p. 911–920.

Singhroy, V.H., Loehr, J.E., and Correa, A.C., 2000, Landslide risk assessment with high spatial resolution remote sensing data, *in* Proceedings, IGARSS 2000, IEEE International Geoscience and Remote Sensing Symposium: Honolulu, Hawaii, v. 6, doi: 10.1109/IGARSS.2000.859620

U.S. Geological Survey, 2018, National Water Information System data (USGS Water Data for the Nation): USGS 13108150 Salmon Falls Creek NR Hagerman ID: doi: 10.5066/F7P55KJN.

Vallet, A., Bertrand, C., Fabbri, O., and Mudry, J., 2015, An efficient workflow to accurately compute groundwater recharge for the study of rainfall-triggered deep-seated landslides, application to the Séchilienne unstable slope (western Alps): Hydrology and Earth System Sciences, v. 19, p. 427–449, doi: 10.5194/hess-19-427-2015

WRCC, 2010, Western Regional Climate Center: HAGERMAN 2 SW, IDAHO Climate records: https://wrcc.dri.edu/cgi-bin/cliMAIN.pl?idhage.

Figures

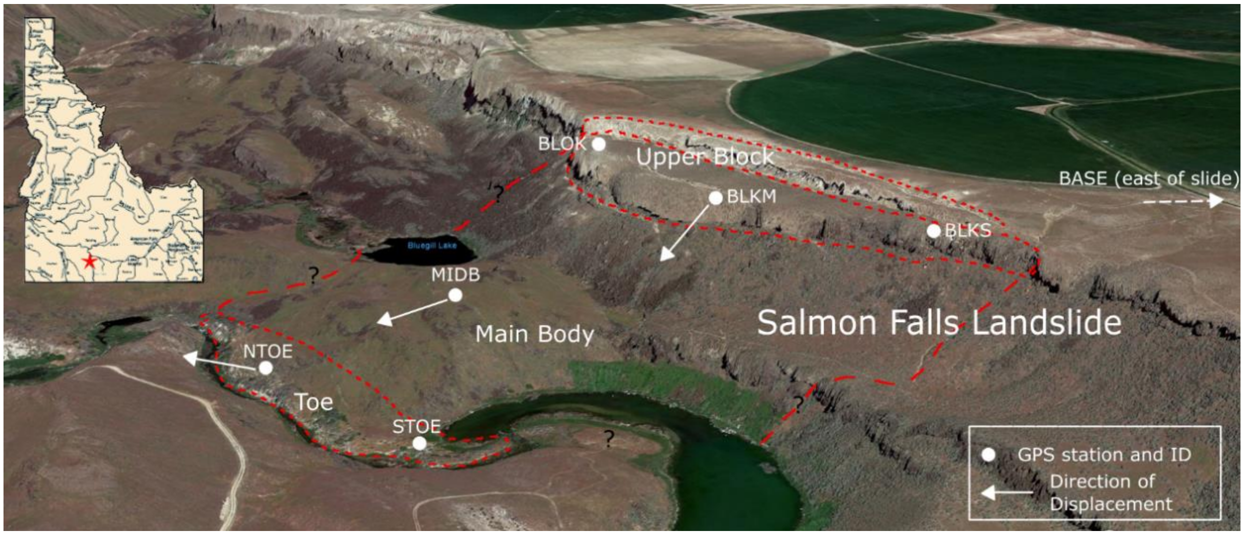

Figure 2.1: Salmon Falls landslide is located in central Idaho, along Salmon Falls Creek, 10 km west of Buhl, ID. It has three distinct kinematic domains: the upper block, middle, and toe. Additionally, three distinct water features are visible here, Salmon Falls Creek, Bluegill Lake, and the canal above the canyon rim.

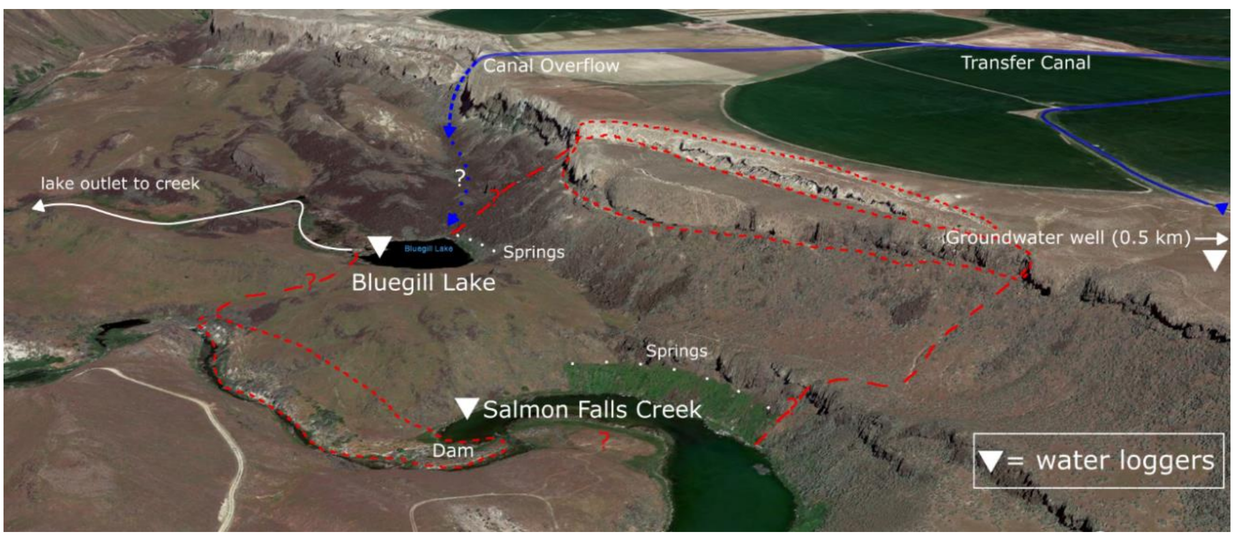

Figure 2.2: The study area has several important water features that contribute to a complex hydrogeologic system. Timing, volume, and spatial relationships between these various water sources and sinks are analyzed for landslide interaction. Not shown here, precipitation contributes both immediately to the study area and also to fluctuations in depth at Salmon Falls Creek, whose drainage area is south of the slide.

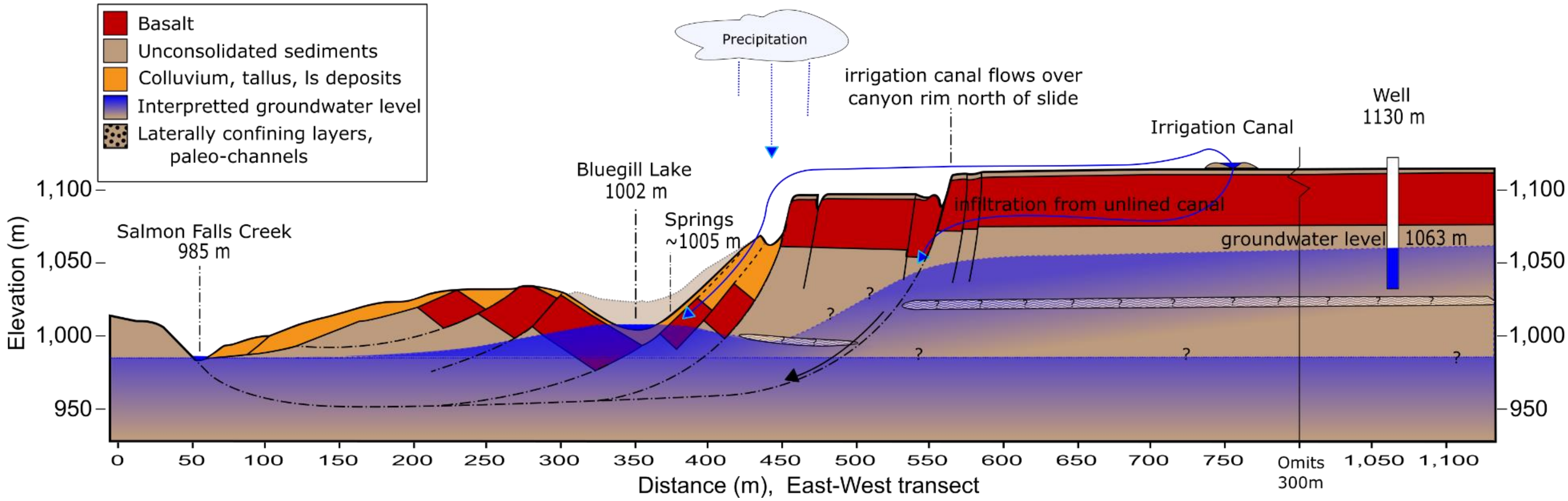

Figure 2.3: One interpretation of cross sectional geology of the Salmon Falls landslide and its hydrogeology. Water levels are highest at the well (right) and decrease towards Salmon Falls Creek (left), likely moving preferentially along horizontally transmissive layers and vertical fractures. Water levels at Bluegill Lake (center) are hypothesized to be representative of elevated saturated water within the slide. Depth of the failure surface is proposed to be as great as 100m at the upper block of the slide and decreasing towards a depth of 30-50m at the middle. Figure based on sections by Necsoiu et al. (2014).

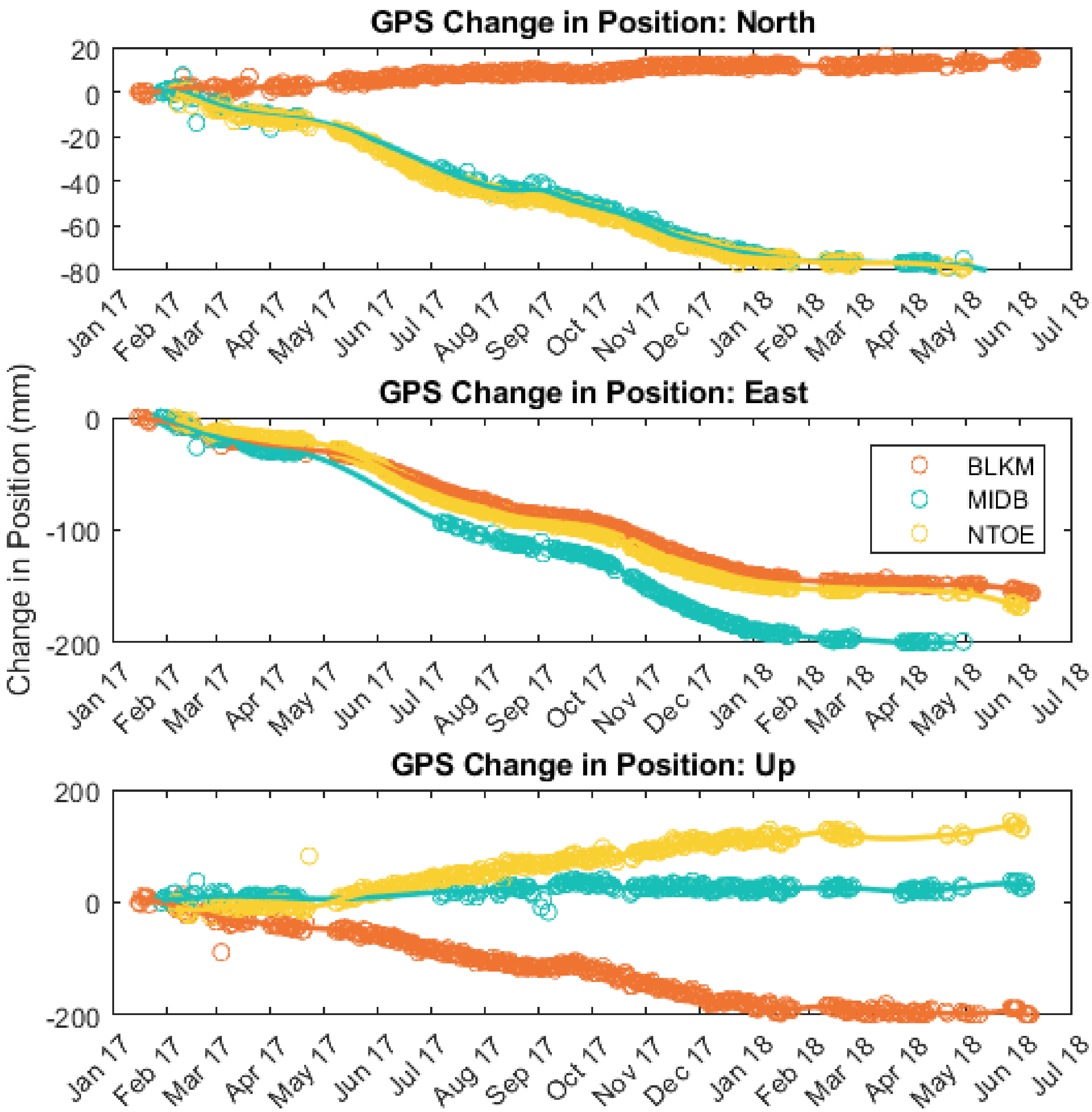

Figure 2.4: Time-series represent 1D motion of each component, North, East, and Up, of the overall 3D motion observed by the GPS stations. The three stations plotted, BLKM, MIDB, and NTOE, represent the major landslide domains: the block, middle, and toe respectively. Solid lines represent the fitted trend model.

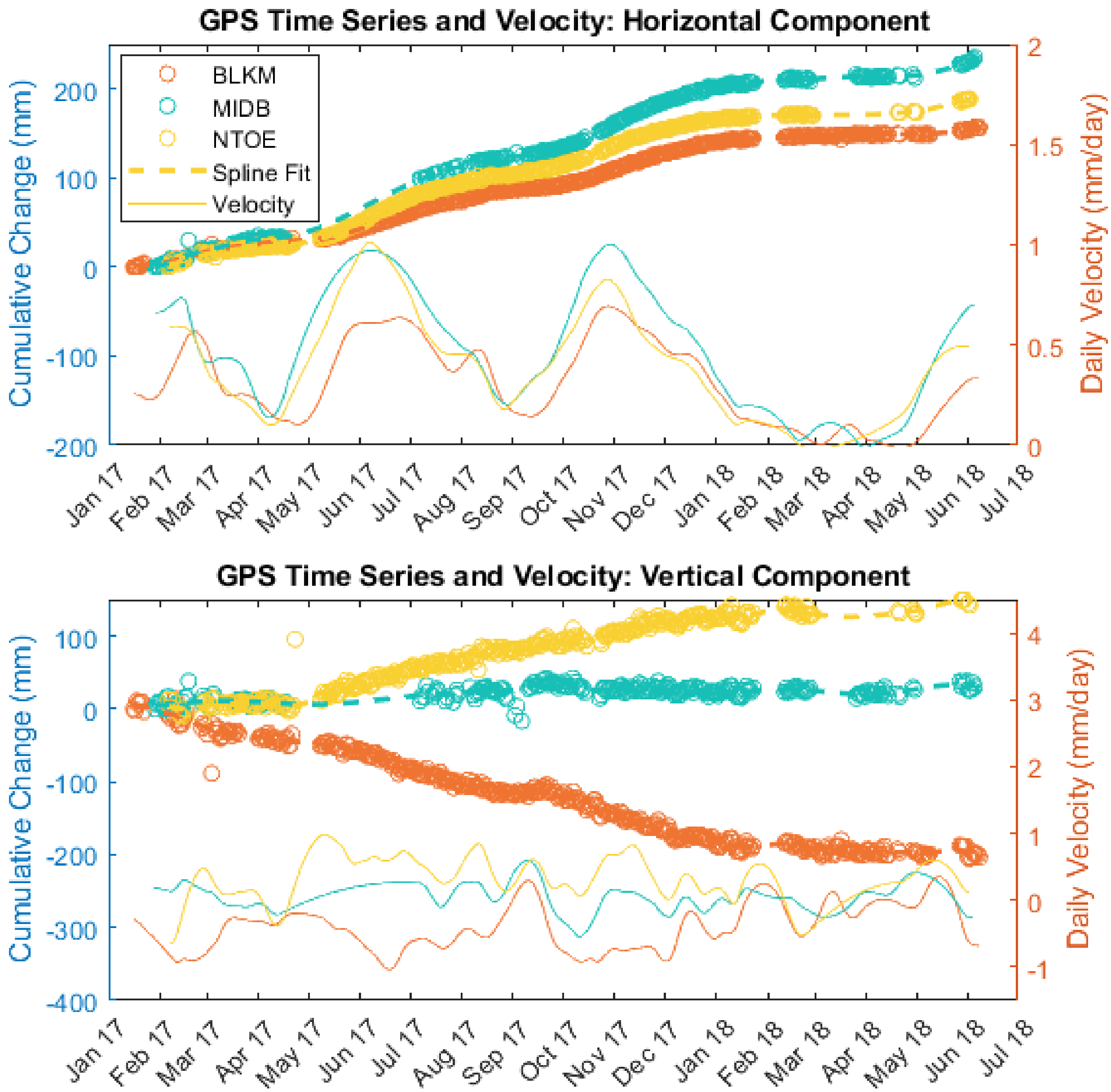

Figure 2.5: Time series of horizontal and vertical vector displacement for each station (left axis) and the time-series of daily velocity calculated from smoothed daily position values (right axis). Note that the vertical velocity signal (bottom) is noisier than the horizontal (top) due to inherent noise in GPS signals, although it exhibits a weakly similar trend. Vertical velocities are absolute to show relative motion regardless of upward or downward direction of movement.

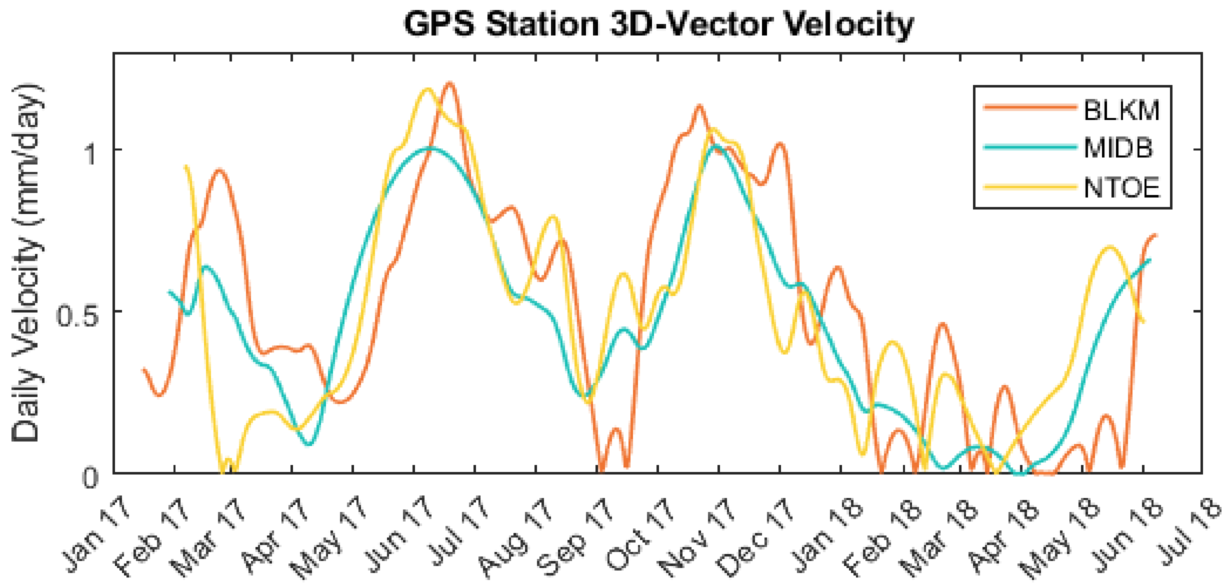

Figure 2.6: Total velocity is the vector sum of horizontal and vertical displacements shown in Figure 2.5. The vertical component of GPS positioning has twice as much inherent error as the horizontal, which carries through to velocity components. Note that the total velocity has a similar overall trend to horizontal velocities in Figure 2.5, which is why we use horizontal velocities in further analysis.

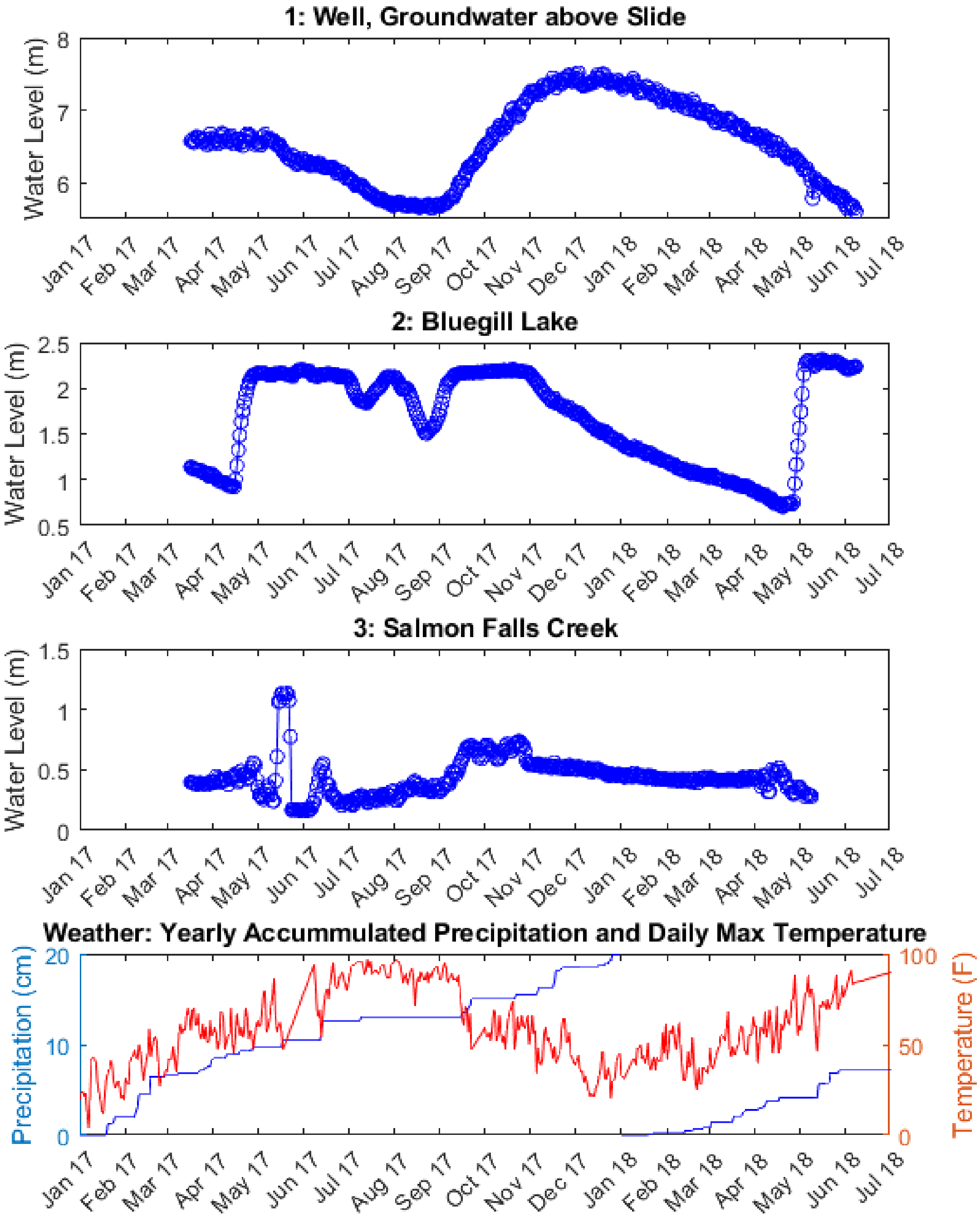

Figure 2.7: Time-series of relative water depth. All depths are relative above the height of the sensor. Note significantly different signals between the well and Bluegill Lake, two water levels which are both suspected to be representative to groundwater depth and are separated by only 0.5km. The start and end of canal irrigation is marked by the red asterisks on the Bluegill Lake plot. The red asterisk on the Salmon Falls Creek plot is the timing of a large streamflow event not related to precipitation but instead dam management. Precipitation accumulates most in the winter to early spring and early fall.

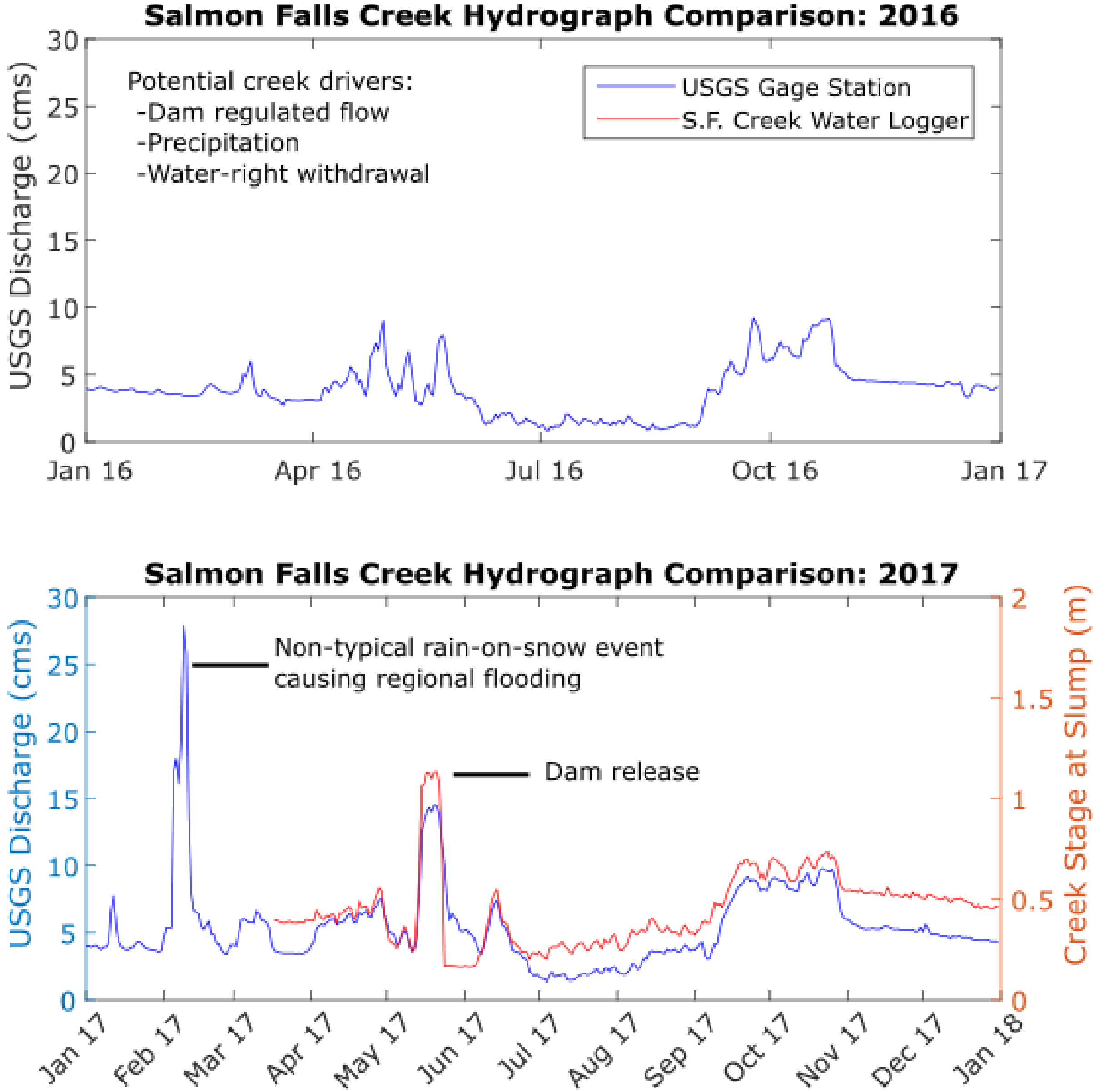

Figure 2.8: The Salmon Falls Creek hydrograph at USGS 13108150 was compared to water loggers installed at the landslide toe in the creek. This revealed that Salmon Falls Creek does have a regular flow pattern, of which 2016 is typical. However, during the GPS survey in 2017, non-typical flows were observed. Note the extremely elevated water levels in February, 2017, which correlates with rain-on-snow that caused severe flooding in the area. A second peak in May is associated with a large volume of water released from Salmon Falls dam.

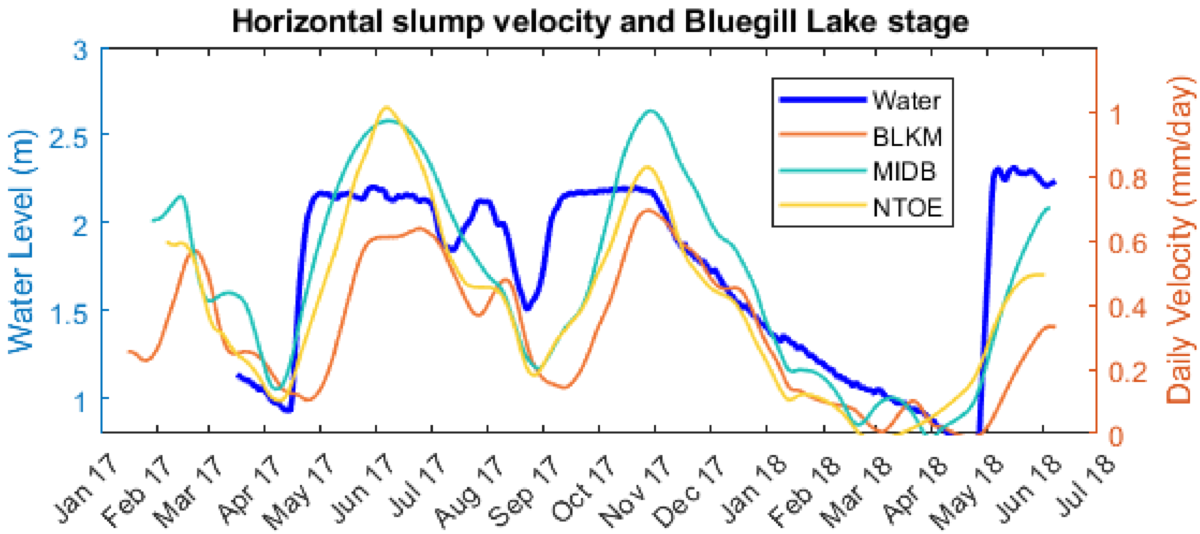

Figure 2.9: Landslide velocity does not appear to be driven immediately by groundwater depth measured above the slide at the well. During some periods, such as May through October, the two signals appear somewhat synchronous. However, during winter and spring months, December through April, water levels are high while landslide velocity is generally decreasing and reaching its minimum. Water measured in the well follows expected behavior of groundwater tables in the area, decreasing in the dry summers and with irrigation withdrawal, and gaining in the winter and spring by precipitation and other sources.

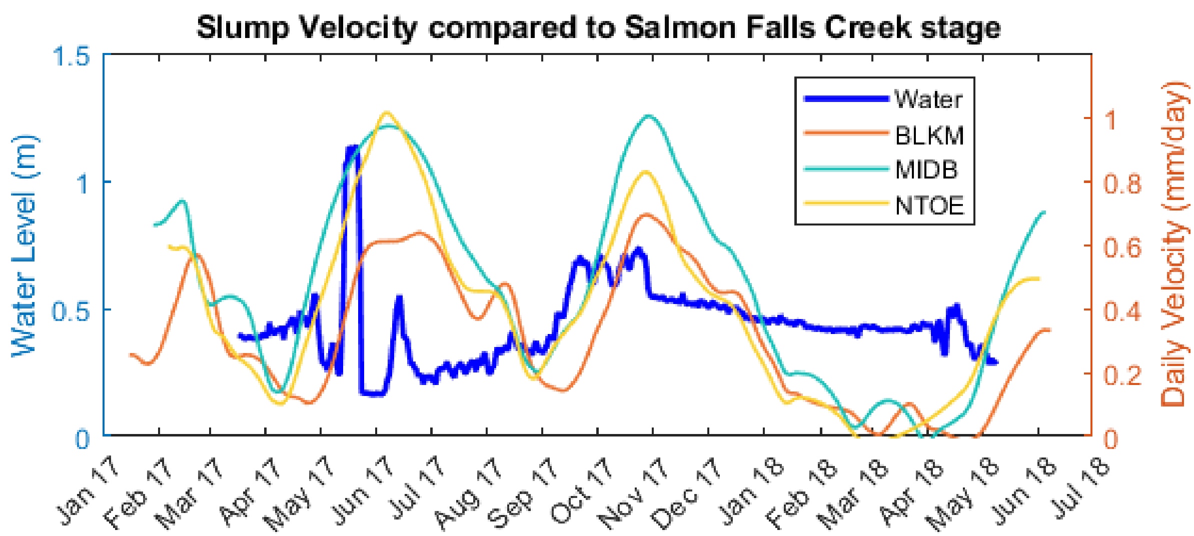

Figure 2.10: Landslide velocity appears to vary independent of water stage in Salmon Falls Creek. However, Salmon Falls Creek may be contributing to the groundwater tables at the toe and middle of the slide, which are also influenced by with other sources. In particular, Salmon Falls Creek appears to rise following precipitation events, another potential driver of groundwater depth in the slide.

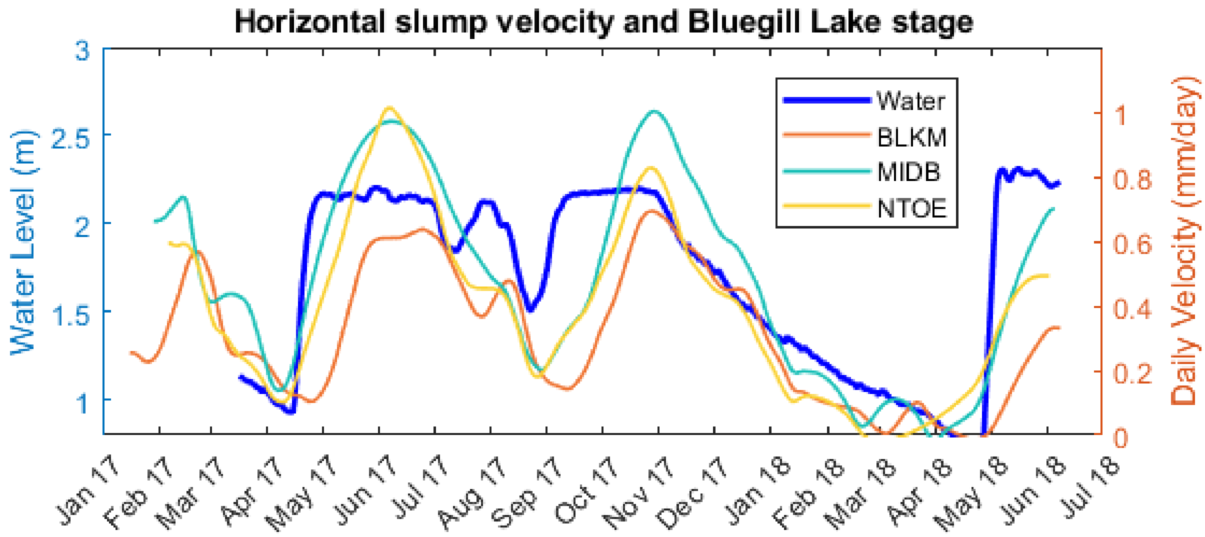

Figure 2.11: Variation in landslide velocity clearly follows water levels expressed at Bluegill Lake, up until Bluegill Lake reaches its maximum capacity at a stage of ~2.2m. At that time, Bluegill lake exceeds its outlet channel height and begins to drain, leaving a plateaued signal at its maximum stage. At this high stage, landslide velocity continues to vary independent of lake water level.

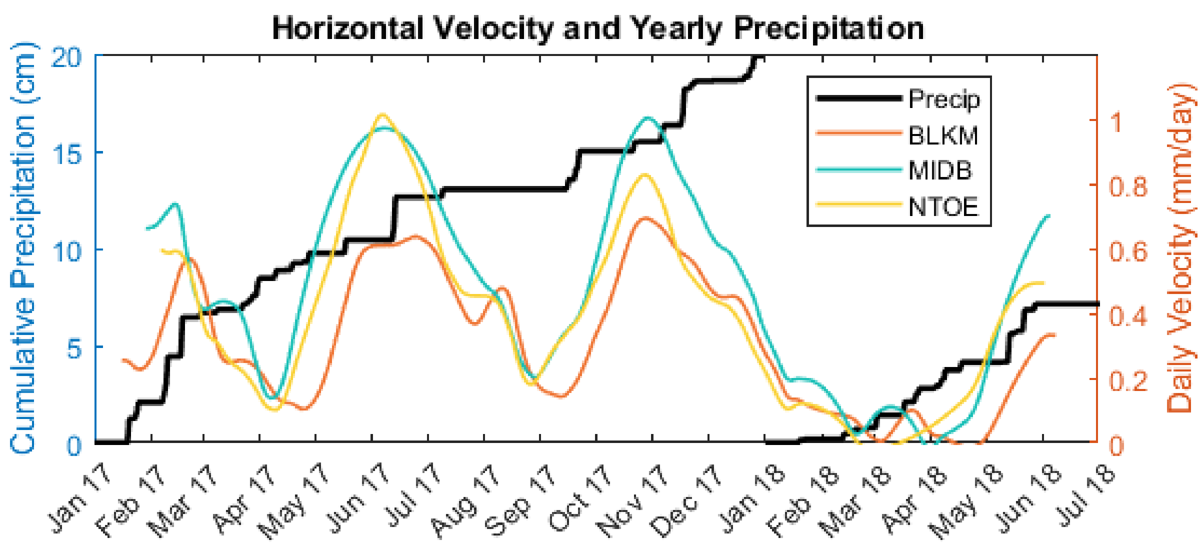

Figure 2.12: Cumulative precipitation across the year was measured 8km to the south at a NOAA station and illustrates that landslide velocity is not entirely driven by these sources. However, one event, an extreme rain-on-snow event in February 2017, accounted for one-third of the yearly water accumulation and caused extensive regional flooding. This event occurred just before the first recorded landslide acceleration in mid-February and may be a potential cause.

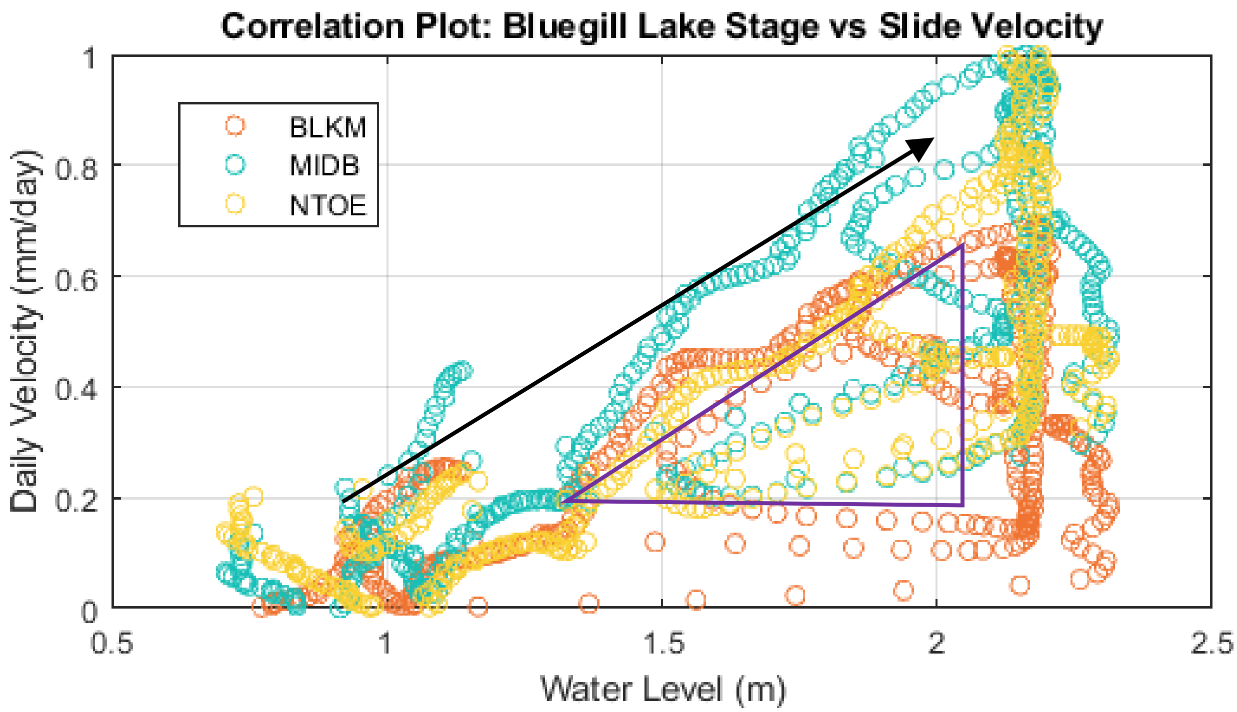

Figure 2.13: Comparison plot of daily velocity vs Bluegill Lake water level. A linear trend is apparent in the data but is obfuscated by the noise in the lower right of the graph. The data in the lower right, highlighted by the triangle, represents landslide velocity fluctuating while water levels in Bluegill Lake are at their maximum and additionally illustrates some unresolved complexities in the relationship. These complexities may include time-variable lag between water source inputs and subsequent rising of the saturated groundwater table.

Salmon Falls Landslide: Annotated Diagram

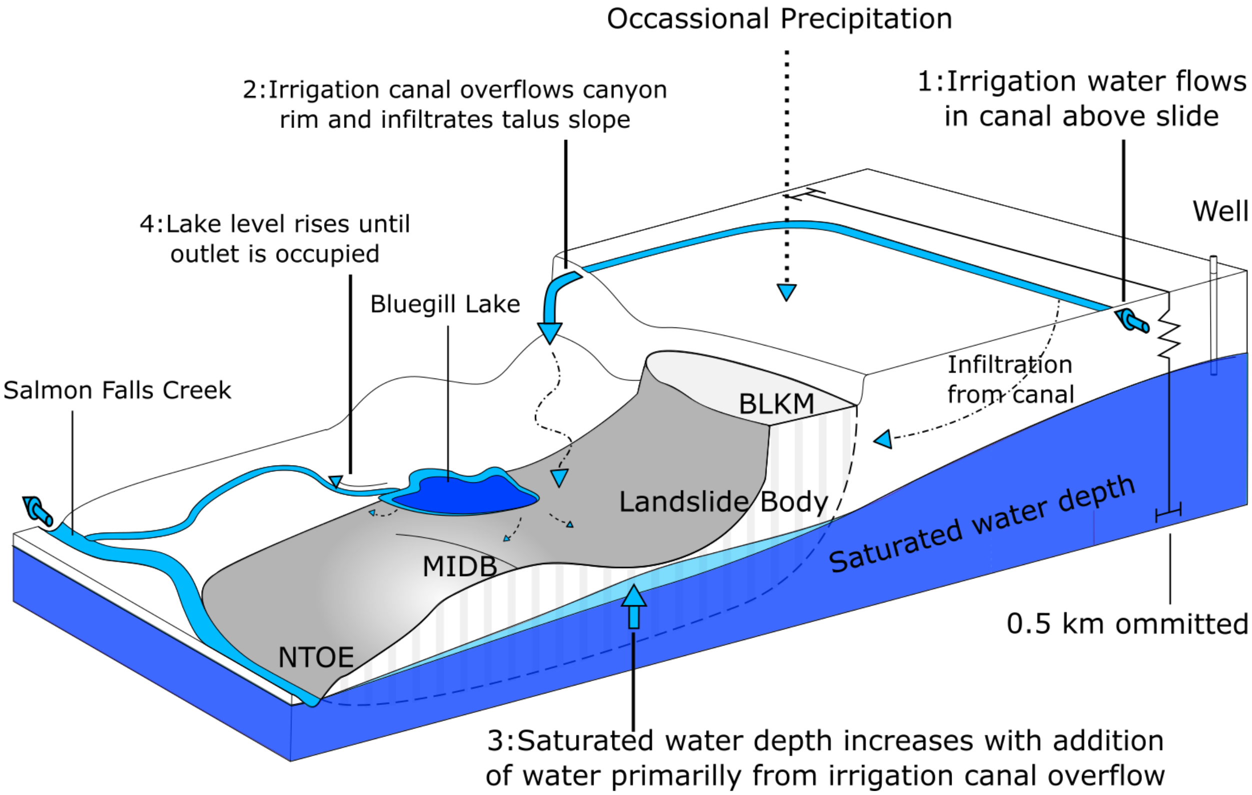

Figure 2.14: Block diagram detailing the interpreted sequence of impacts irrigation has on Bluegill Lake and local groundwater at the Salmon Falls landslide. Numbered steps detail the sequence of events leading to increased slide velocity. Infiltrated water from canal losses and normal precipitation are interpreted as minor influences on slide velocity. Similarly, stream flow and regional groundwater are also interpreted as minor influences on slide velocity.

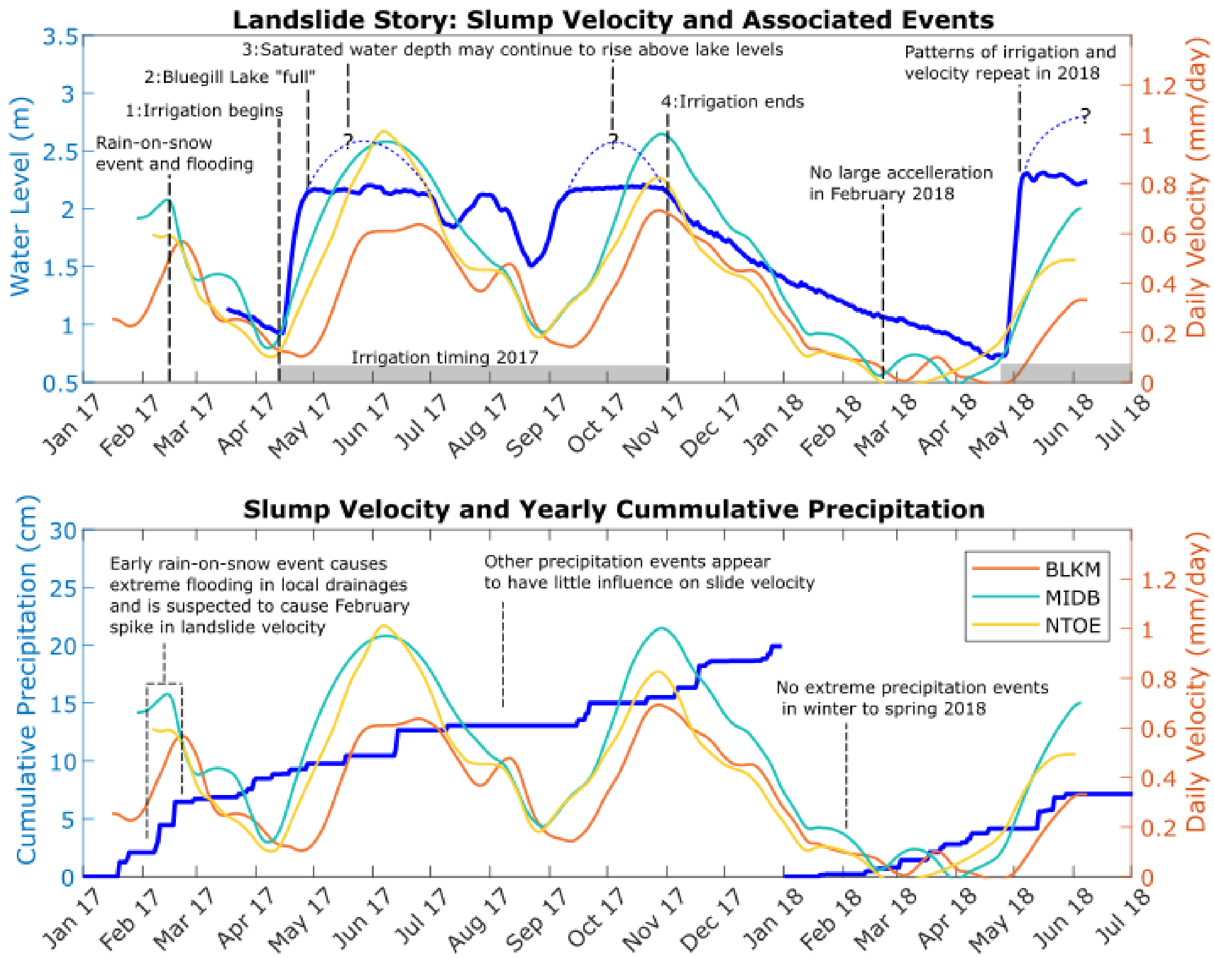

Figure 2.15: Interpretation of groundwater influence on the Salmon Falls landslide. Note that visual correlation between lake water levels and landslide velocity is high until Bluegill Lake reaches its maximum storage capacity (3) and overflows through the outlet channel. At high water depths, we interpret that saturated depth in the slide increases beyond lake levels, increasing pore-pressure and preceding the trends in landslide velocity (4). Timing of irrigation water availability highly correlates to seasonal water level trends in Bluegill Lake (2 and 5), except in the early spring when a non-typical precipitation event lead to flooding and likely elevated groundwater levels (1).

Tables

	Table of fit values: MATLAB Curve Fitting Toolbox, Smoothing Spline, Smoothing Parameter = 0.001											
Vector	BLKM		BLKS		BLOK		MIDB		NTOE		STOE	
Componen	r^2	RMSE	r^2	RMSE	r^2	RMSE	r^2	RMSE	r^2	RMSE	r^2	RMSE
North	0.9651	0.5984	0.9825	0.7332	0.9955	0.9937	0.9983	0.9468	0.9977	0.9375	0.9981	1.1424
East	0.9993	0.9365	0.9831	0.6927	0.993	0.9239	0.9991	1.6667	0.9995	0.8955	0.9986	0.8803
Up	0.9905	4.3836	0.5735	3.847	0.9935	5.69	0.7908	5.052	0.9859	4.4304	0.9826	4.7417
Horizontal	0.9993	0.9308	0.9913	0.6782	0.9993	0.9647	0.9997	1.10093	0.9995	0.9795	0.9991	1.0532
Total	0.9966	3.2755	0.9266	1.9277	0.9962	4.8402	0.9989	2.0068	0.9978	2.484	0.9956	3.1744

Table 2.1: Goodness of fit values for non-parametric models of daily time-series GPS displacements. Each vector component, N, E, and Up was modelled separately along with a combined model for Horizontal vector (East+North) and a total vector (East+North+Up). Non-parametric models produce a “spline” between components and are weighted on a smoothing parameter that controls the percentage of values that must be fit. A value of 1 fits 100% of the points (a new line between every point), whereas a value of 0 only attempts to fit the first and last values (a straight line). A value of 0.001 is used, which reduces noise in daily positions.

Station ID	Daily Velocity [mm/day]				Yearly [cm/yr] Velocity
	Mean	Min	Max	Std	
BLKS	0.1	-0.2	0.4	0.1	3.2
BLKM	0.6	-0.1	1.2	0.3	22.9
BLOK	0.9	-0.1	1.6	0.4	32.0
MIDB	0.6	0.1	1.0	0.3	20.8
STOE	0.5	0.0	1.0	0.3	17.7
NTOE	0.6	0.0	1.2	0.3	20.4

Table 2.2: Velocity estimates calculated from daily displacement values obtained from the non-parametric fitting model. BLKM, MIDB, and NTOE are highlighted, the three representative stations used in regression analysis. BASE is not listed, because its motion has already been differrenced from the signal of the other six stations. Precision of the GPS instrumentation is ±1-3mm on daily positions. Daily velocities shown here are calculated from daily displacement smoothing models, which reduce the inherrent noise in daily positions. Therefore, statistical measures here are not based on instrumentation results, but represent the modelled values.

Chapter 3: Conclusion

3.1 Summary

This project aimed to observe the behavior of Salmon Falls landslide, particularly yearly patterns of slide velocity, and determine whether local water sources were responsible for this interaction. Saturated groundwater above a failure surface in a hillslope is a known driver of landslide activity based on the force of pore-water pressure (Van Asch et al., 1999). Previous GPS surveys in 2003 recorded a single, large magnitude acceleration in landslide velocity that occurred during the dry, summer season in Idaho. The counterintuitive observation suggested additional drivers may be acting on the landslide such as irrigation water (Dorsch, 2004; Chadwick, Dorsch, et al., 2005). We explored this hypothesis by re-surveying the slide with continuous, high-precision GPS and paired hydrologic measurements from 2017-2018.

Correlations between time-series of landslide velocity and local water level observations revealed a complex hydrogeologic system which regulates landslide motion (Figure 2.14 and 2.15). Local groundwater levels are interpreted as being high within the landslide body and emerge from mid-elevations on the body of the slide. The local groundwater table was found to be the most likely source for Bluegill Lake as well as multiple springs. The water level at Bluegill Lake fluctuates seasonally, coinciding with the timing of water flow from irrigation canals along the canyon rim of the slide. The lake reaches its maximum water level shortly after irrigation begins in early summer and the water overtops its outlet channel and begins to flow into Salmon Fall Creek. GPS velocity time-series showed nearly continuous movement on the landslide pronounced by three distinct accelerations that lasted 4 months on average and fluctuated over an order of magnitude from 0.1 mm/day to 1 mm/day. Two of these accelerations coincided with fluctuations of water level in Bluegill Lake and the third coincided with an extreme rain-on-snow event in early spring of 2017.

From these observations, we proposed a two-part model could be formed for the relationship between saturated groundwater depth and landslide velocity. At low levels, Bluegill Lake represents saturated water depth within the slide and exhibits a positive, linear correlation to landslide velocity. As saturated water levels rise, Bluegill Lake rises until it has reached its maximum height, which is controlled by elevation of its output channel. The second part of the model represents behavior after saturated water depth exceeds levels at Bluegill Lake. Once Bluegill Lake has occupied its outlet, its maximum height is controlled by flow from the outlet. During these times, landslide velocity continues to rise and fall along a simple parabolic function which matches temporally with lake levels anytime lake level falls below the maximum depth (Figure 2.15). As such, we proposed that saturated water depth is still increasing within the slide body beyond the maximum height of Bluegill Lake.

This study suggests that the Salmon Falls landslide does follow known water-hillslope interactions and pore-water pressure relationships. We found that this deep-seated, slow-moving, rotational slide can be sensitive to relatively small fluctuations in groundwater depth, which vary annually by approximately 1 m. Additionally, behavior observed on the slide did follow the general kinematic behavior described by previous authors, although patterns of acceleration on the landslide did not match those of the earlier 2003 survey. It is difficult to determine if historic hydrologic conditions in the landslide match the current observations because no local groundwater records exist. However, regional climate records suggested that conditions were relatively dry in 2003 compared to wet conditions in 2017-2018 and this could have caused both regional groundwater depths to change as well as cause a shift in irrigation schemes that would affect local groundwater levels. Landslides in the Salmon Falls area and surrounding regions have previously been shown to be sensitive to anthropogenic water sources. Unlined irrigation canals are the principal sources, and our research confirms these processes are at work in Salmon Falls Creek (Chleborad and Powers, 1996; Farmer, 2003).

Landslide are known to be affected when saturated with water, and this study adds a new case study to this literature as well as giving regionally significant information on landslide mechanics. Landslides are a common actor in canyon formation within the greater geologic system of the Snake River Plain and analogous regions, such as eastern Washington and Oregon (Bareither et al., 2012; Ely et al., 2012; Markley, 2013; Othus, 2008; Safran et al., 2015). This information will be critical to land managers who are responsible for informed decisions about placement and construction of canal structures which may be adjacent to sensitive features such as active landslides. Lining of canals structures and preventing overflow into sensitive hillslope areas could slow movement on and possibly delay formation of mass-wasting in these areas.

3.2 Future Work

3.2.1 Motivation

This project aimed to both understand if landslide kinematics had evolved over the age of the slide and to determine if known landslide drivers could explain the previously observed patterns in landslide velocity. We found that saturated water depth is well correlated to landslide velocity, however we required a multi-part model based on a single year of data to explain the behavior. Similarly, we found landslide kinematics to be consistent, however temporal variation in landslide velocity was inconsistent with previous work. The previous survey had noted only a single, large acceleration during fall, whereas we found three distinct acceleration events which occurred in the spring, early summer, and then mid fall, as well as a distinct period of undetectable movement in spring 2018.

3.2.2 Landslide Hydrology

We found that Bluegill Lake was a reasonable estimator of saturated depth and pore-pressure, but only when Bluegill Lake was below its maximum depth. Importantly, this shows that saturated groundwater depth near Bluegill Lake are representative of landslide velocity at low lake depths, so we may be able to take advantage of the elevated water depth to install a shallow well on the slide near the lake that would measure groundwater depth directly.

Although water level in Bluegill Lake appears to be a good indicator for landslide behavior, this is driven by an influx of irrigation water. However, this connection is based purely on time-correlation of changes in Bluegill Lake with the onset of flow in the irrigation canal and a single discharge and water loss measurement in the canal. Exact timing and volume of water flow from the canal to the landslide body is unknown. To address this, in 2018 we installed water loggers in the canal above the landslide and near the canyon rim to record the exact timing of flow onset and discharge. This data will improve our knowledge of the timing and volume of introduced to the landslide area.

3.2.3 Landslide Kinematics

The main goal of studying landslide kinematics was to determine if slide motion was exhibited similar spatial and temporal patterns to the original 2003 survey. Spatial patterns were observed to be consistent, and we concluded that characterization of the upper, middle, and toe blocks was accomplished by the current network. At the conclusion of this study, we additionally decided to pare down the network from its redundancies and now have a single GPS station monitoring each landslide domain. Temporal relationships between slide domains were revealed, which were not apparent in the original survey. We found 3 distinct acceleration events throughout the year, which occurred nearly simultaneously at each station. This contrasts with the original survey which showed only a singly acceleration in a yearlong period and may suggest that landslide behavior has changed in the interim 15 years.

3.3 Conclusion

We found that expected saturation-sliding velocity relationships hold true in the Salmon Falls slide, and these relationships are driven by the local augmentation of groundwater tables by irrigation water inputs. However, our work is limited by surficial water observations that necessitated a two-part model to explain relationships and relies on considerable interpretation of a single year of data. Continued observation of the landslide over several years would extended the range of data over which the model could be tested, and the hydrologic story could be validated. Recent installation of monitoring stations along the irrigation ditch will improve our estimations of it water contribution and proposed shallow wells in the landslide may aid in direct measurement of slide saturation. GPS stations have been acquired for continued semi-permanent installation on the landslide at the four main stations used in our analysis, NTOE, MIDB, BLKM, and BASE, reducing the study complexity to its necessary components. The main factor in the continuation of the study will be the supply of fresh, enthusiastic field hands to collect data and maintain instrumentation at the site.

Chapter 3 References

Van Asch, T.W.J., Buma, J., and Van Beek, L.P.H., 1999, A view on some hydrological triggering systems in landslides: Geomorphology, v. 30, p. 25–32, doi: 10.1016/S0169-555X(99)00042-2.

Bareither, C.A., Edil, T.B., and Benson, C.H., 2012, Investigation of White Bluffs Landslides in Washington State: GeoCongress 2012: State of the Art and Practice in Geotechnical Engineering, 2012, p. 546–555, doi: 10.1061/9780784412121.057

Chadwick, D.J., Dorsch, S.J., Glenn, N.F., Thackray, G.D., and Shilling, K., 2005, Application of multi-temporal high-resolution imagery and GPS in a study of the motion of a canyon rim landslide: Photogrametry and Remote Sensing, v. 59, p. 212–221, doi: 10.1016/j.isprsjprs.2005.02.001.

Chleborad, A.F., and Powers, P.S., 1996, Slope map and locations of irrigation-induced landslides and seepage areas, Hagerman Fossil Beds National Monument, Idaho: U.S. Geological Survey Open-File Report 96-258, 1 p., http://pubs.er.usgs.gov/publication/ofr96258.

Dorsch, S.J., 2004, The Geologic framework, movement history and mechanics of the Salmon Falls Landslide, Twin Falls County, Idaho [M.S. thesis]: Idaho State University, 138 p.

Ely, L.L., et al., 2012, Owyhee River intracanyon lava flows: Does the river give a dam? Geological Society of America Bulletin, v. 124, p. 1667–1687, d oi: 10.1130/B30574.1

Farmer, N., 2003, Hagerman Valley landslides triggered by land-use change endanger lives, and destroy natural and cultural resources (Hagerman Valley Fossil Beds National Monument, NPS, Idaho): Journal of the Japan Landslide Society, v. 40, p. 341–343, doi: 10.3313/jls.40.4_341.

Markley, C.E., 2013, Characterization of mass wasting through the spectral analysis of LiDAR imagery: Owyhee River, Southeastern Oregon [M.S. thesis]: Central Washington University. 60 p.

Othus, S.M., 2008, Comparison of Landslides and Their Related Outburst Flood Deposits, Owyhee River, Southeastern Oregon [M.S. theis]: Central Washington University, 146 p.

Safran, E.B., O'Connor, J.E., Ely, L.L., House, P.K., Grant, G.E., Harrity, K., Croall, K., and Jones, E., 2015, Plugs or flood-makers? the unstable landslide dams of eastern Oregon: Geomorphology, v. 248, p. 237–251, doi: 10.1016/j.geomorph.2015.06.040.